1-1-2005

Fluorescence Prediction through Computational Chemistry

Daniel Craig Lathey

Fluorescence Prediction through Computational Chemistry

A Thesis Presented to
The Graduate College of
Marshall University

In Partial Fulfillment
Of the Requirements for the Degree of
Masters of Science
Chemistry

By
Daniel Craig Lathey

Marshall University
Huntington, West Virginia
May, 2005

Abstract
Fluorescence Prediction through Computational Chemistry

By: Daniel Craig Lathey

With the growing demand for diverse fluorescent dyes, it is imperative to find a more efficient methodology by which to synthesize dyes. Our research group has found a computational method that can efficiently predict the optical properties of a molecule before it is synthesized. By evaluating different semi-empirical methods, we have found a way to predict the fluorescence maxima. With the new ability of Hyperchem 7.5 to geometrically optimize a molecule in an excited state, we can predict not only the absorption maxima, but we can also predict the fluorescence maxima within 25 nm of the actual fluorescence.

With this new ability to use computational chemistry to replace the traditional laboratory research, we can remove the tedious process of trial and error, and focus on compounds that have the desired optical properties that we need.

Acknowledgements

I would like to thank Dr. Morgan for inspiring this thesis and research. I would also like to thank Dr. Price for his advice and coaching on the matters of computational chemistry and the basics of the quantum mechanics that drives the theories and equations. Thanks to Dr. Burcl for agreeing to be on my thesis committee and his guidance through this research. Most of all I wish to thank the entire Chemistry Department for all of the help, use of facilities, and the wealth of knowledge I now possess as I leave Marshall University.

Table of Contents

List of Figures

List of Tables

Chapter 1: Past and Present Research

Introduction

Our group has patented a technique for synthesizing a family fluorescent molecules called pyridoimidazolium cations[1,2] or PIC's for short (PIC's, Figure 1). The importance and application of fluorescent dyes has grown exponentially over the years in many fields of study[1]. Presently, there are over 44,000 fluorescent dyes available commercially[6] and these dyes are only part of an ever increasing collection of molecules needed in many fields, including medical, analytical, and biochemical.[1] Along with the ever-expanding uses for different fluorescent molecules, a need for more dyes tailored to each application also continues to grow. For example, dyes may only be needed to specifically stain certain organelles or certain tissues while in the presence of other biological structures. For this reason, an extensive library of dyes with different optical properties needs to be developed to meet this demand. With the traditional methods of synthesizing molecules in hopes of producing the desired optical properties, the process of producing molecules with a wide variety of emission maxima becomes extremely expensive in terms of time.

The PIC's that are prepared by multi-step synthesis, can require several days in the lab and may provide less than desirable yields; therefore this research can become very expensive in terms of time and money spent in the lab. In attempts to find a better protocol, computational chemistry was utilized to predict the fluorescence of molecules prior to the effort of synthesizing them. With a focus of perfecting an inexpensive way to predict the emission maxima of several compounds before synthesis, not only can synthesis of molecules with less than adequate optical properties be avoided, but also, a

method by which to study and compare the factors that can influence fluorescence can be utilized.

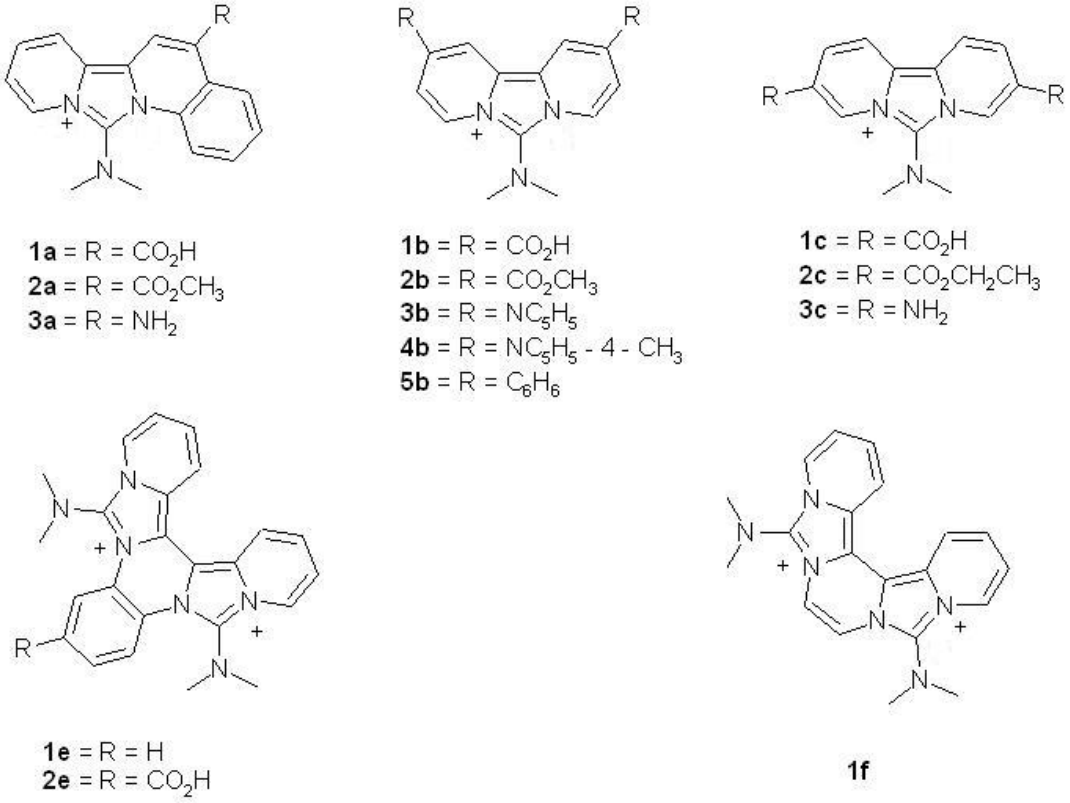

Figure 1: Synthesized PIC's – These pyridoimidazolium cations were synthesized through the work of Dr. Morgan's group [1,2]

Theory of Fluorescence

When a molecule absorbs a photon, it is raised to a higher energy state producing a molecule that is in a rovibronic electronic state. While in this excited state, the molecule may undergo an internal conversion relaxing to a slightly lower excited state of the same spin without emitting any radiation. From this lower excited state, the molecule returns directly to the ground state releasing energy in the form of light. This process can

be shown in a simplified version of the Jablonski diagram (Figure 2). Based on the Frank-Condon principle, which states that nuclei do not move appreciably during a transition between electric states, all transitions can be depicted as vertical lines. Because of the internal conversion, the energy needed to excite the molecule is always higher than the energy emitted and the difference between the excitation and emission maxima is called the Stoke's shift (Figure 3).

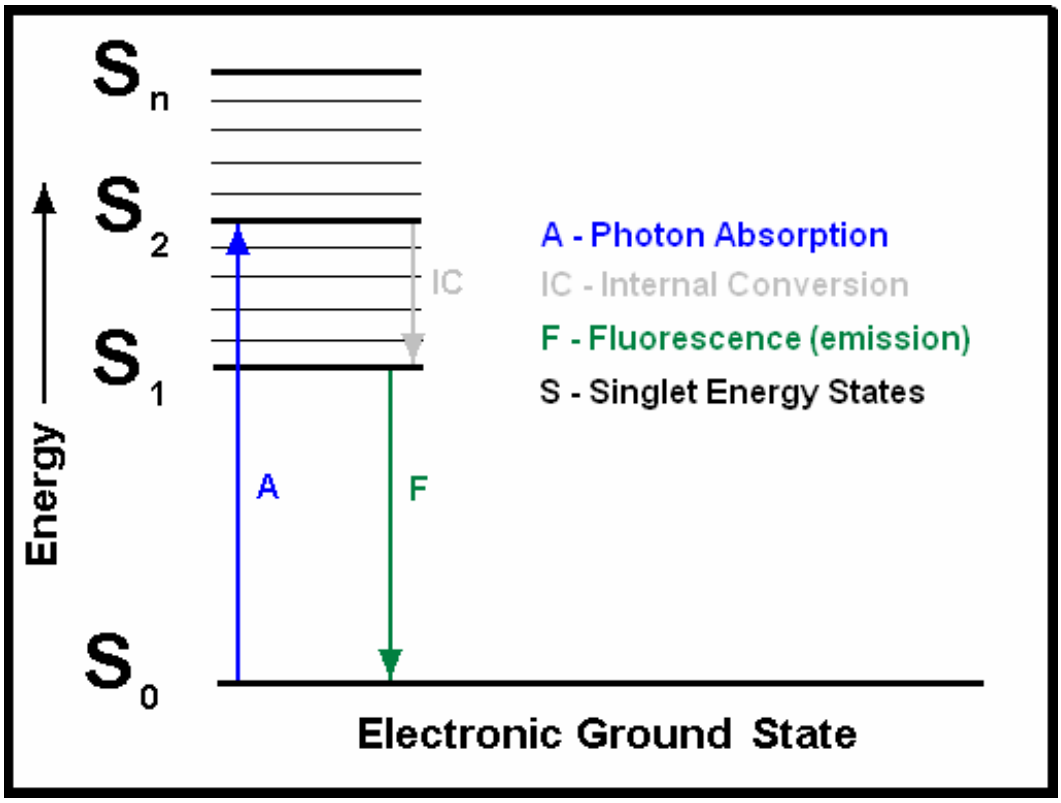

Figure 2: Jablonski Diagram – Diagram showing the process by which fluorescence is produced. As a photon enters the molecular system, the molecule is excited to a higher electric state. According to the Frank-Condon principle, these transitions can be depicted as vertical lines. After the initial excitement, the molecule can undergo a radiationless internal conversion to a slightly lower excited state. From this state the molecule returns to the ground site relaxing and releasing energy in the form of fluorescence.

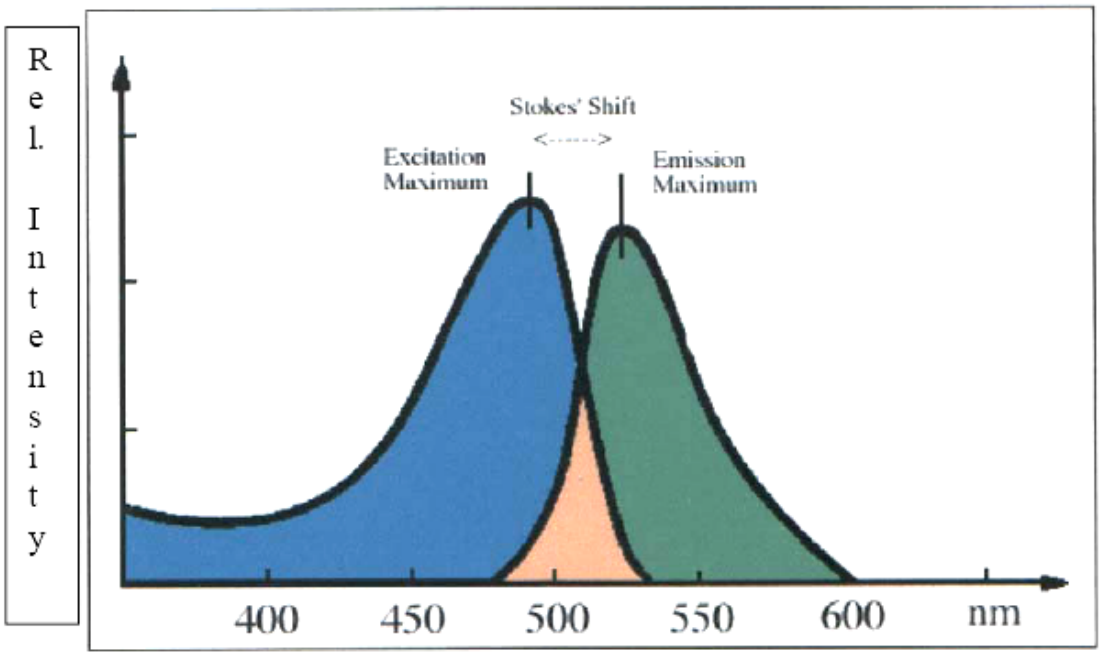

Figure 3: Stoke's Shift[2] – This diagram depicts the difference between excitation and emission maxima, called the Stoke's Shift.

Prediction of Fluorescence through Computational Chemistry

By introducing different functional groups at various positions on the aromatic rings of the PIC's, emission maxima can be altered (Table 1). The prediction of fluorescence spectra through computational chemistry is a new field of study attempting to discover a more systematic and inexpensive method of producing fluorescent dyes. However, in past works such as the Fabian[3-5] and the Rambacher[2] papers, certain limitations have presented themselves in simulating complex molecular systems such as PIC's. In light of this, more reliable and accurate method of predicting fluorescence spectra of highly complex molecules has been found by utilizing different levels of semi-empirical theory to simulate spectra.

Past Research

There are two approaches to modeling spectroscopic features, *ab initio* and semi-empirical methods. Traditionally, chemists have found that *ab initio* techniques are entirely too expensive in terms of time because they use the Schrödinger equation without any further experimentally obtained approximations. Semi-empirical methods use parameters from experimental data, simplifying the approximation of the Schrödinger equation and lowering the expense of the calculation.[2] In two of the Fabian papers,[4,5] *ab initio* calculations were compared to various semi-empirical methods and the less expensive semi-empirical methods were actually found to be more accurate than the *ab initio* in the prediction of both absorption and emission spectra. Therefore, in the past, semi-empirical methods have been used because they have shown to be both inexpensive and sufficiently accurate for many applications.[3-5]

To obtain sufficiently accurate calculations, proper geometric optimization of the ground and singly states is crucial. In the Fabian paper[3-5], the group used MOPAC 6.0 and VAMP 4.40 program packages utilizing AM1 methods that proved to be an accurate method of optimizing for the purpose of determining electronic spectra. However, under AM1 conditions, a few of the more complex molecules failed to converge in the excited state and their electronic spectra were unobtainable.[3-5]

Rambacher, from our research group, chose to use Hyperchem 6.0 because of its availability, its Microsoft Windows compatibility, and its user-friendly format. In his paper, Rambacher's results were reasonably accurate, but the work lacked any theoretical rational as to why it was successful. However, with Hyperchem 6.0, there were several limitations. For example, in version 6.0, calculating geometric optimization of a

molecule in the excited state was not an option. This is a crucial step in determining the emission spectrum of a molecule. Also, instead of relying on the accuracy of the AM1 semi-empirical method from previous research to geometrically optimize molecules, Rambacher used the most general form of molecular mechanics, MM+.[2] This method treats atoms as Newtonian particles interacting through a potential energy function depending on bond lengths, bond angles, torsion angles, and nonbonded interactions; however, it does not take into account the effects of electron density or localization, therefore providing a less accurate optimization.

A New Approach to the Problem of Optimizing the Excited State

In attempts to obtain a more accurate and theoretically sound method of fluorescence spectral prediction, Hyperchem 6.0 was upgraded to version 7.5 which provided an option to run a geometric optimization of a molecule in an excited state using semi-empirical methods. As in the Fabian work,[3-5] the AM1 method to geometrically optimize the ground state of the molecule was used. However, this became problematic in many of the more complex cases when molecules were in their excited states and would not geometrically converge. In attempts to correct this problem the ZINDO/1 semi-empirical method was used for geometric optimization of molecules in the excited state. This method was chosen because it contains parameters designed for singly excited molecules. The ZINDO/S method has proven to be extremely accurate in calculating electronic transition energies and intensities both in absorption and emission spectra.[2-5] Hyperchem suggests using ZINDO/1 for excited state geometric optimization and not ZINDO/S. Other works have also used ZINDO/1 for geometric optimization of large organic molecules with great success.[8-14] This method of excited state geometric

optimization worked well for the purposes of this research and allowed all of the molecules, irrespective of size, to converge.

Based on the methods from both the Fabian and Rambacher papers, the ZINDO/S semi-empirical method was used to calculate the molecules' transition energies and simulate both the absorption and emission spectra. However, one problem still became evident; Hyperchem was basing all calculations with the assumption that the molecules were in vacuo and while Fabian's work showed little solvent effects,[3] our aromatic molecules were more complex and quite different with an overall positive charge. PIC's had the possibility of being affected by solvent conditions to a rather large degree. To correct this issue, .a correction for the difference of the solution matrix would have to be taken into consideration. Two different approaches were taken. In the first approach, a list of absorption and emission data of solution data from the Rambacher paper[2] was taken and compared directly to the data obtained through computational chemistry. In the second approach, experimental data was analyzed by first comparing the spectra of four molecules frozen at 77K with the in vacuo calculations to obtain an empirical fitting parameter and then comparing those calculations with spectra of the same solutions at room temperature to obtain a solvent correction factor.

As a test of this new approach, synthesis of two new molecules was attempted (Figure 4). With these molecules, their experimental fluorescence could be compared to the calculated prediction.

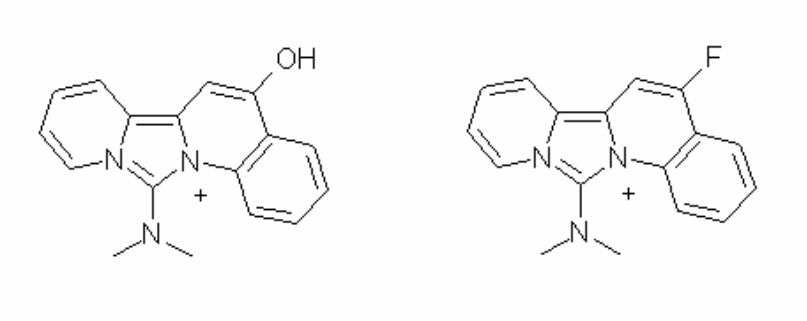

Figure 4: 4-hydroxy-2-(2-pyridyl) quinoline and 4-fluoro-2-(2-pyridyl) quinoline PIC's

Chapter 2: Computational Method

Calculations of the Ground State

To avoid any complications with translation of structure, all of the molecules were drawn in Hyperchem 7.5 instead of importing a structure from another graphics program as was done in the Rambacher paper.[2] A step by step account of running these calculations in Hyperchem is located in Appendix B. For geometric optimization, the semi-empirical method was set to AM1 and all molecules were set to a charge and spin multiplicity of 1 under the options and the CI method set to "None." The structures were then geometrically optimized with an RMS gradient of 0.01 using the Polak-Ribiere method. The cycle limit was then set to 1000 to allow for enough time to converge. The Polak-Ribiere method was used instead of the Eigenvector Following as was done in the Fabian papers[3-5] because the Eigenvector Following was unable to allow the PIC's to converge.

After the geometric optimization was complete, a log file was started to record subsequent calculations. Single-point calculations were then performed using ZINDO/S parameters with the CI method set to "Singly Excited" and the orbital criterion set to 5 occupied and 5 unoccupied orbitals. An electronic spectrum was then generated and the transitions saved in the log file. The log file was stopped.

Calculations on the Singly Excited State

After the ground-state simulation was completed, the molecule was geometrically optimized using ZINDO/1 with the same orbital criterion and the CI method still set to singly excited. The only method available in Hyperchem for excited geometric optimization is "Conjugate Directions" and this optimization takes an average of one and

a half hours to complete on our system (see experimental for details). Optimization was performed on the excited state to simulate internal conversion.

After the optimization was complete, the semi-empirical method was set back to ZINDO/S using the same options as for the single point calculation on the ground state. A new log file was created in order to capture the calculations. As before, a single point calculation was performed followed by the generation of an electronic spectrum and the log file was closed.

Experimental

All computations were performed with Hyperchem 7.5 on a Sony Vaio desktop PC with Windows XP, a 2.66 GHz Intel Pentium 4 Processor, and 268 MB of RAM. All data and graphs were calculated and analyzed on Microsoft Excel XP. All the experimental emission spectra for the PIC's used in this approach were measured on a Spex Fluorolog TAU-3.

Results

Approach #1

All the experimental excitation and emission spectra for our PIC's used in this approach were provided by the Rambacher paper.[2] All calculations and simulated spectra were performed on molecules in vacuo and the experimental data was collected from the spectra of molecules in solution. The main goal of this approach was to find an inexpensive and reliable way to simulate and predict fluorescence spectra for PIC's in fluid solution. To achieve this, a plot of the solution experimental data vs. the calculated results was generated to obtain an empirical fitting parameter, or EFP.

Absorption Calculations

In all simulated spectra, the last two significant peaks were taken because they best mimicked the spectra shape, as shown in Figure 5. The wavelength of maximum absorption used was taken as a weighted average of the last two significant peaks (the peaks that best mimicked the spectra shape) in the ZINDO/S log file from the electronic spectrum of the AM1 geometrically optimized ground state. Table 1 shows the data before being corrected by the empirical fitting parameter from the absorption correlation graph (Figure 6). The average percent error before incorporating the empirical fitting parameter was 4.07% with the greatest margin of error with compounds 1a, 2a, 1e, and 2e being off by approximately 30 nm and compounds 1b and 2b being off by approximately 20 nm.

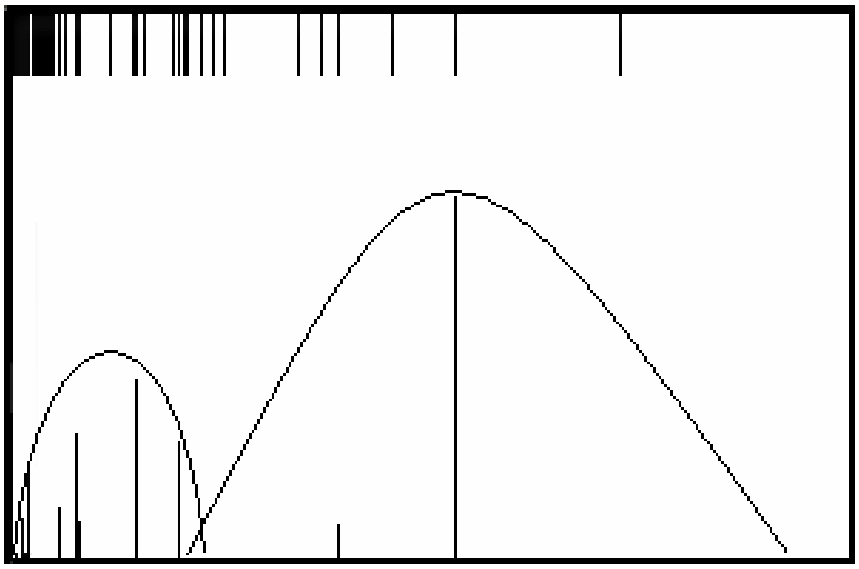

Figure 5: Simulation spectra from Hyperchem 7.5. The last two peaks fit under what looks to be where the drawn curve would be. This is the reason these were the only ones analyzed by a weighted average. All peaks in the other grouping were lower than the excitation spectral maximum and if there was a third peak in any of the graphs under the curve, they were always insignificant because of there low intensities.

Compound	Calculated Absorption (nm)	Experimental Absorption (nm)	% Error
1a	404.3	433.7	6.78%
2a	403.7	434.1	7.01%
1b	414.9	433.1	4.21%
2b	414.9	434.1	4.41%
3b	444.7	443.4	0.29%
4b	463.6	467.9	0.91%
5b	421.4	419.17	0.54%
1e	445.5	477.29	6.65%
2e	444.4	477.31	6.90%
1f	451.4	465.32	2.99%

Table 1: Calculated vs. Experimental Absorption Data collected before incorporating the empirical fitting parameter.

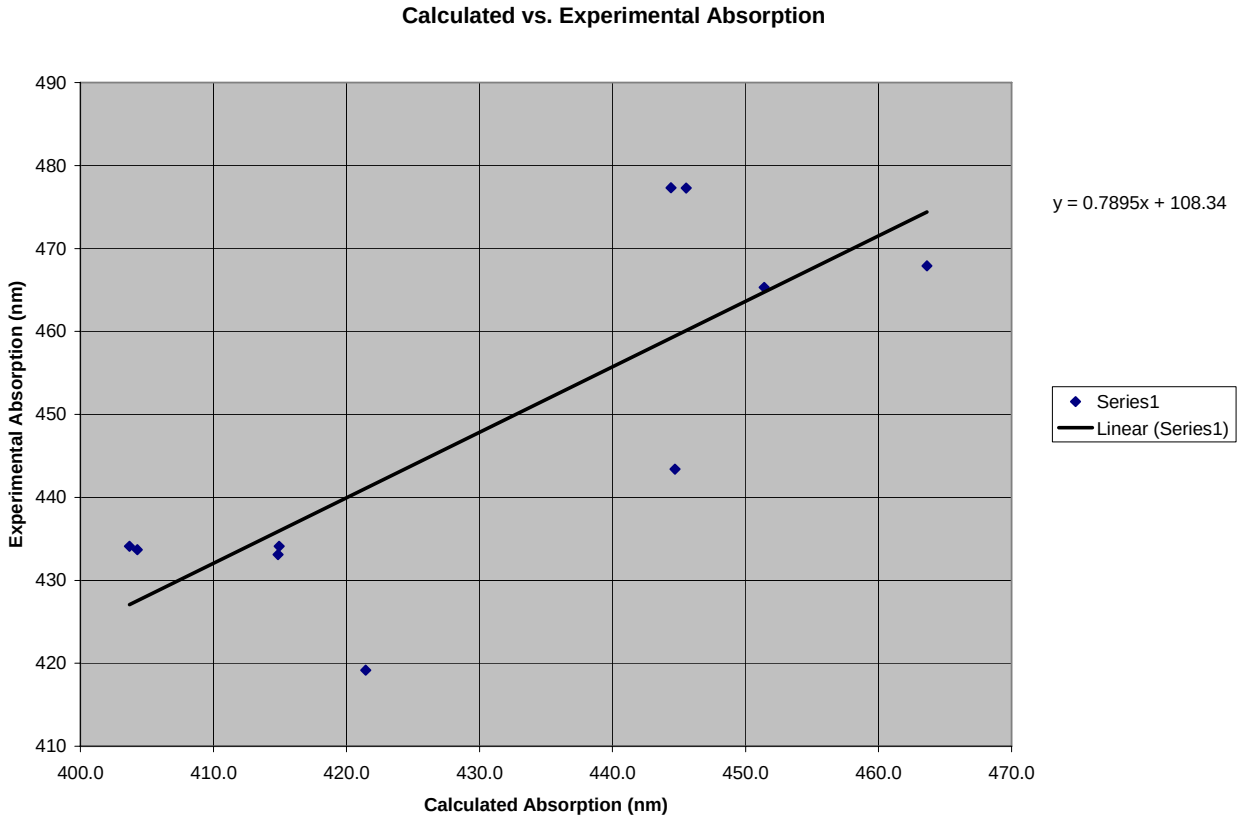

Figure 6: Absorption Linear Correlation Graph Incorporating the EFP

By using the linear equation y = 0.7895x +108.5 obtained from the correlation graph (Figure 6), the data in Table 2 was obtained. The average percent error was lowered to 2.19%. The compounds with the highest deviation were 3b, 5b, 1e and 2e being off by approximately 16 – 21 nm.

Compound	Corrected Calculated Absorption (nm)	Experimental Absorption (nm)	% Error
1a	427.5	433.7	1.43%
2a	427.1	434.1	1.62%
1b	435.9	433.1	0.64%
2b	435.9	434.1	0.42%
3b	459.4	443.4	3.61%
4b	474.4	467.9	1.38%
5b	441.1	419.17	5.23%
1e	460.1	477.29	3.60%
2e	459.2	477.31	3.80%
1f	464.7	465.32	0.13%

Table 2: Calculated vs. Experimental Absorption data after incorporating the empirical fitting parameter found from the Linear Correlation Graph

Emission Calculations

The calculated emission wavelengths were found by taking a weighted average of the last two significant peaks in the ZINDO/S log file from the electronic spectrum of the excited state which was geometrically optimized with ZINDO/1. Table 3 shows the data before being corrected by the emission linear correlation graph (Figure 7). The average percent error before the empirical fitting parameter was incorporated was 8.42%.

Compound	Calculated Emission (nm)	Experimental Emission (nm)	% Error
1a	456.0	494	7.68%
2a	462.1	505	8.49%
3a	522.9	573	8.74%
1b	469.4	524	10.43%
2b	580.6	533	8.93%
3b	625.5	571	9.55%
4b	606.1	626	3.17%
5b	547.8	540	1.45%
1e	480.8	550	12.58%
2e	490.6	550	10.80%
1f	490.6	550	10.81%

Table 3: Calculated vs. Experimental Emission data collected before incorporating the empirical fitting parameter.

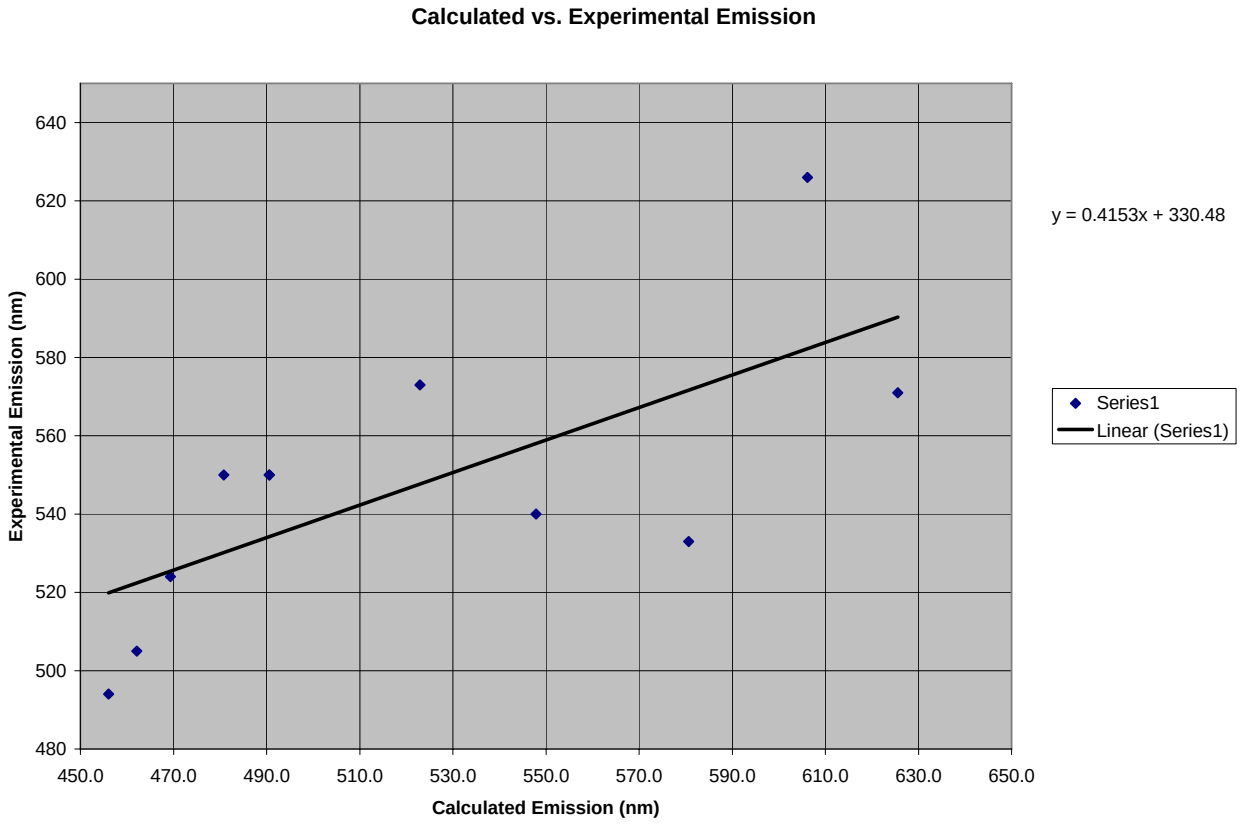

Figure 7: Emission Linear Correlation Graph

By using the linear equation y = 0.4153x + 330.48 obtained from the correlation graph (Figure 7), the data in Table 4 were obtained. With this correction average percent error was lowered to 3.97% and the calculated spectra maxima was more accurate being within approximately ± 15 nm. The most deviation was with compound 4b being off by 43 nm.

Compound	Corrected Calculated Emission (nm)	Experimental Emission (nm)	% Error
1a	519.9	494	5.24%
2a	522.4	505	3.45%
3a	547.7	573	4.42%
1b	525.4	524	0.27%
2b	571.6	533	7.24%
3b	590.3	571	3.37%
4b	582.2	626	7.00%
5b	558.0	540	3.33%
1e	530.2	550	3.61%
2e	534.2	550	2.87%
1f	534.2	550	2.87%

Table 4: Calculated vs. Experimental Emission data after incorporating the empirical fitting parameter found from the Linear Correlation Graph

Approach #2

The only compounds used with this approach were compounds 1a, 2a, 1b, and 2b because 77K emission data were available (Figures 8-15). The main goal of this approach is to incorporate not only an empirical fitting parameter, but also to find a solvent correction factor. This factor will be used to correlate between emission spectra in vitrified matrix, as compared to fluid solution. Calculations from the simulated fluorescence spectra were first plotted against the experimental spectra from the molecules in a 50-50 methanol/ethanol frozen matrix at 77K (Figure 16) to get an

empirical fitting parameter. Table 5 shows the data before being corrected by the empirical fitting parameter (Figure 16).

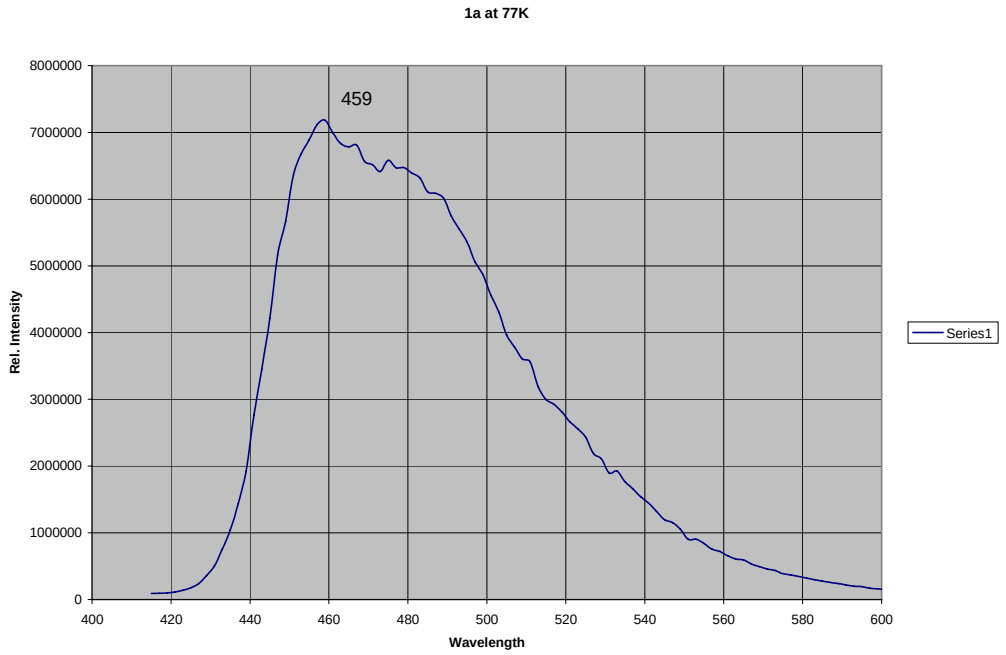

Figure 8: Emission spectra of PIC 1a at 77K. The point displayed shows λ_{max} at 459 nm.

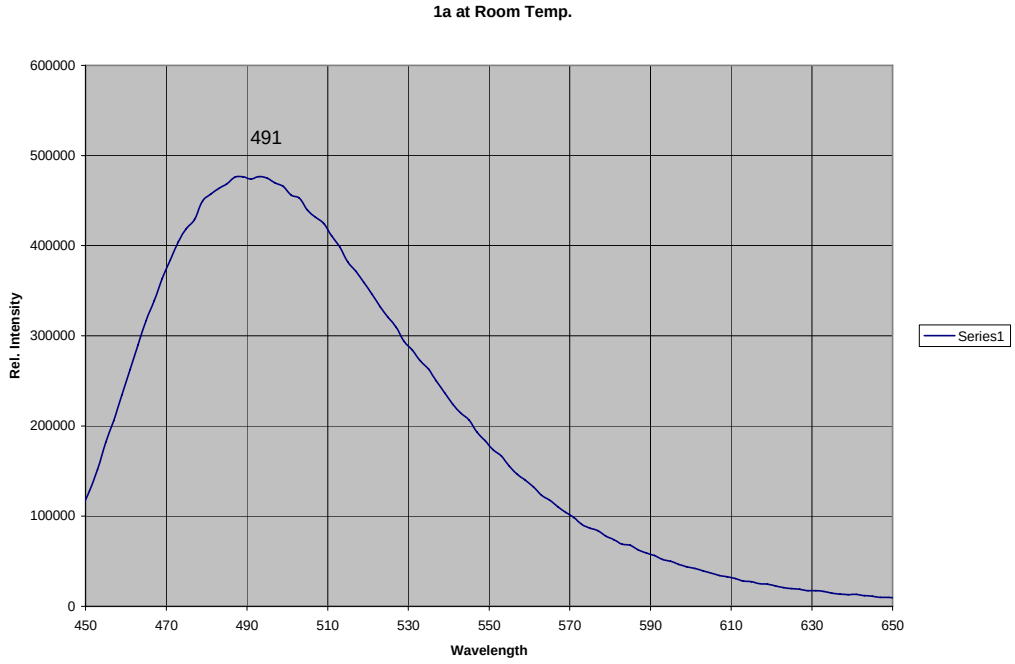

Figure 9: Emission spectra of PIC 1a at room temperature. The point displayed shows λ_{max} at 491 nm.

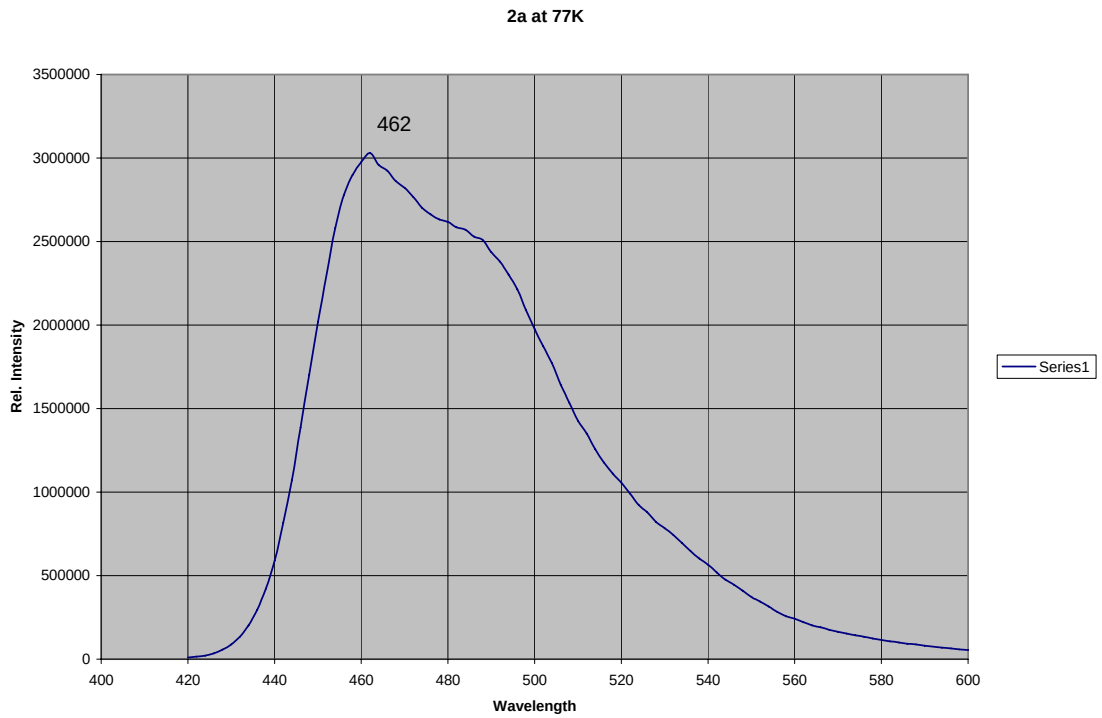

Figure 10: Emission spectra of PIC 2a at 77K. The point displayed shows λ_{max} at 462 nm.

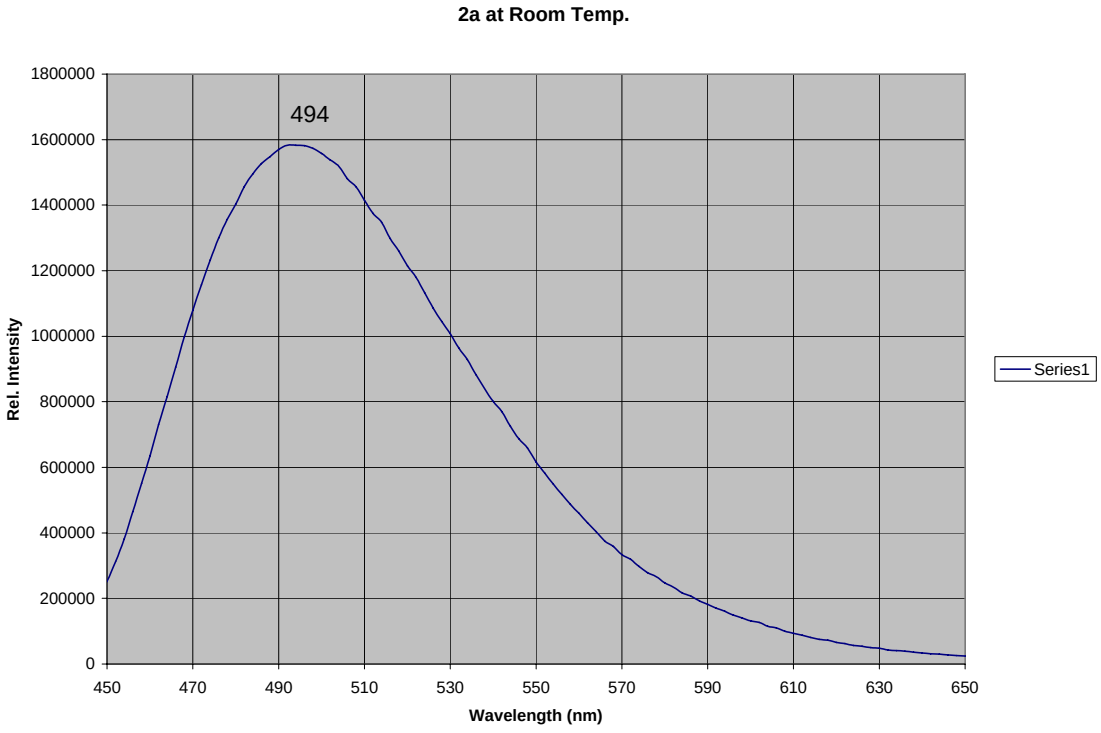

Figure 11: Emission spectra of PIC 2a at room temperature. The point displayed shows λ_{max} at 494 nm.

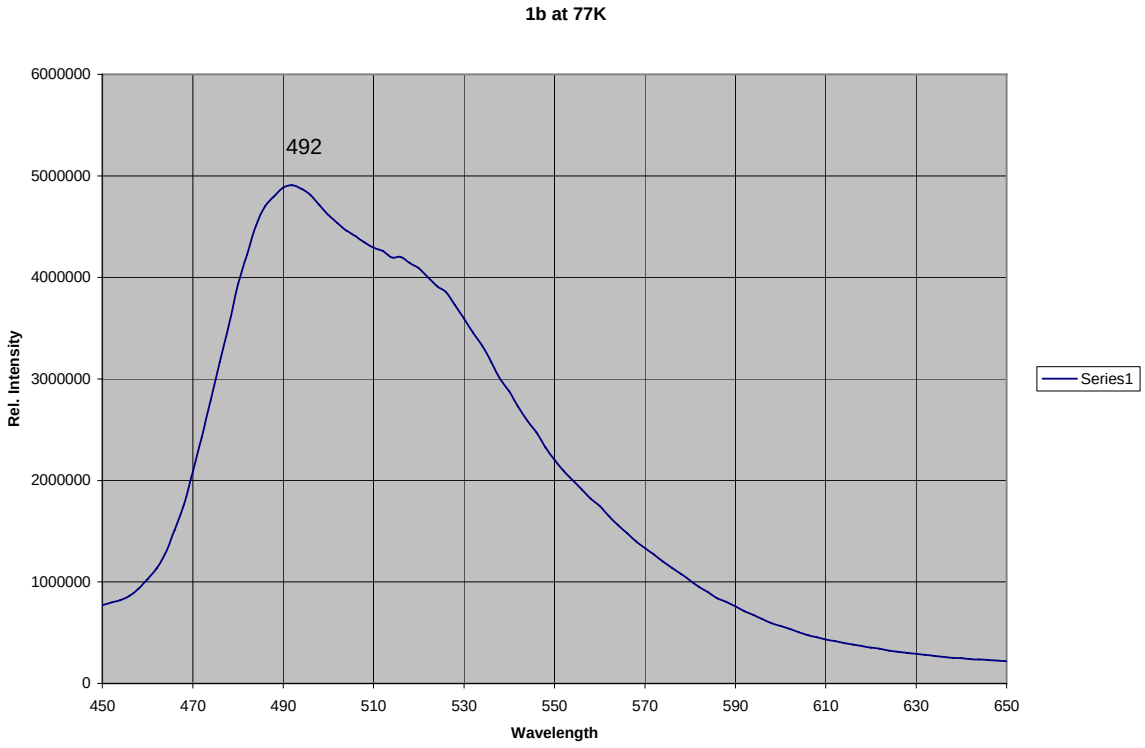

Figure 12: Emission spectra of PIC 1b at 77K. The point displayed shows λ_{max} at 492 nm.

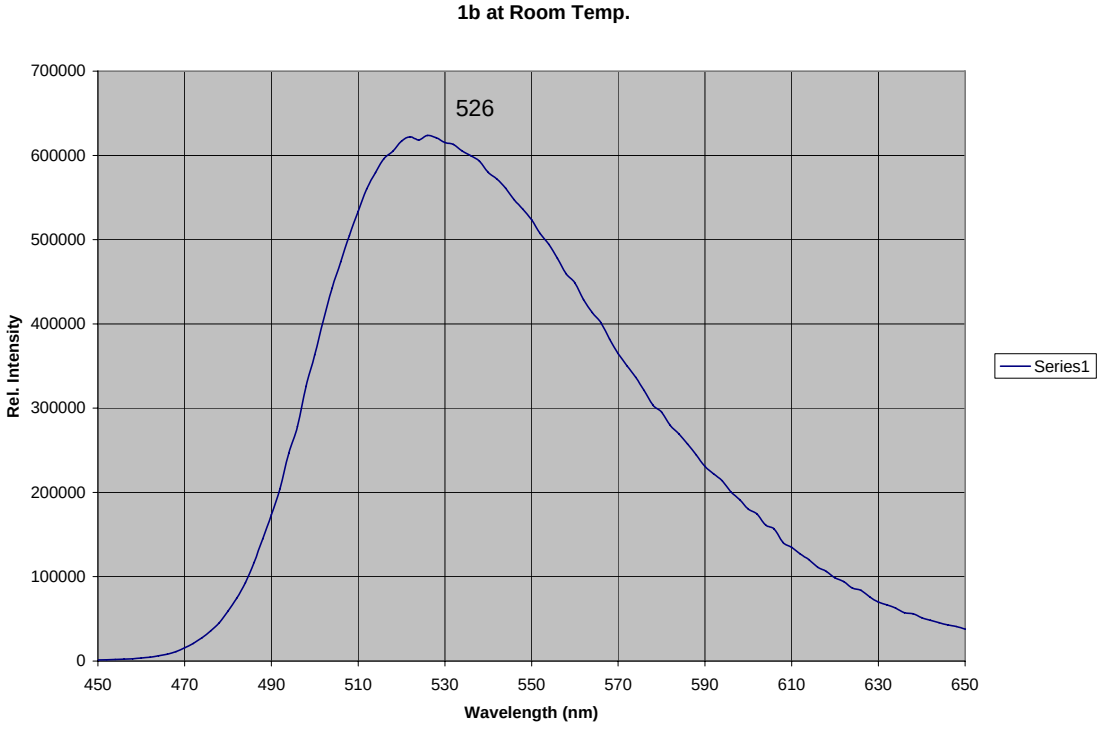

Figure 13: Emission spectra of PIC 1b at room temperature. The point displayed shows λ_{max} at 526 nm.

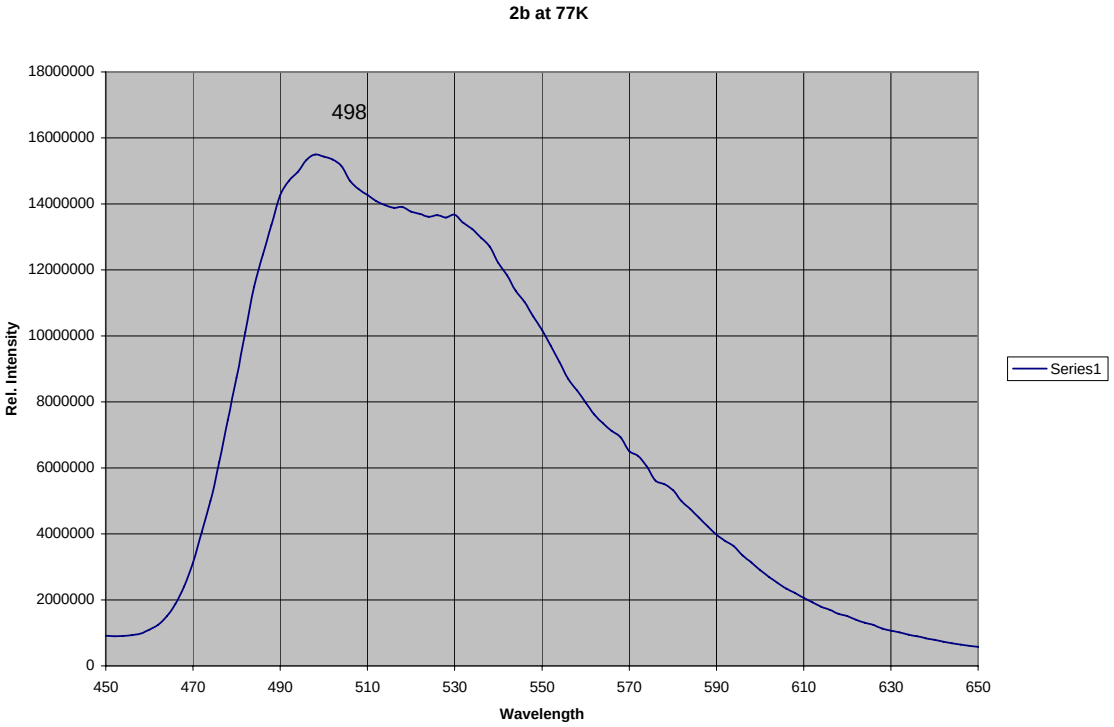

Figure 14: Emission spectra of PIC 2b at 77K. The point displayed shows λ_{max} at 498 nm.

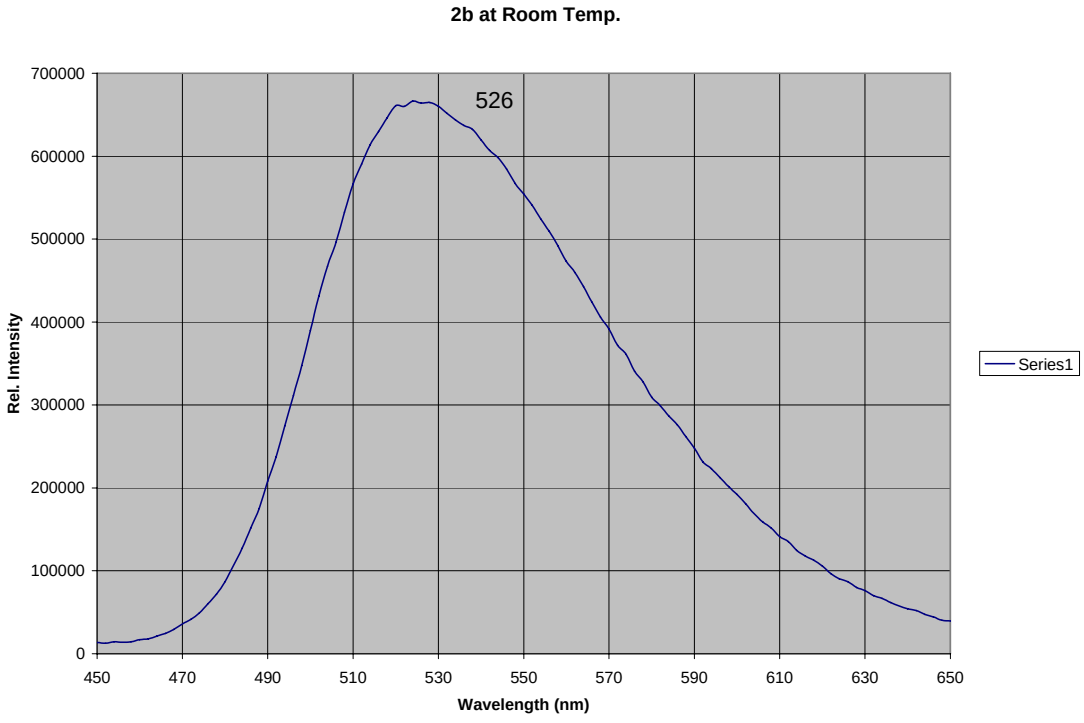

Figure 15: Emission spectra of PIC 2b at room temperature. The point displayed shows λ_{max} at 526 nm.

Compound	Calculated Emission (nm)	Experimental Emission (nm) @ 77K	% Error
1a	456.0	459	0.65%
2a	462.1	462	0.00%
1b	469.4	492	4.59%
2b	580.6	498	16.59%

Table 5: Calculated vs. Experimental Emission Data @ 77K before incorporating the EFP and SCF

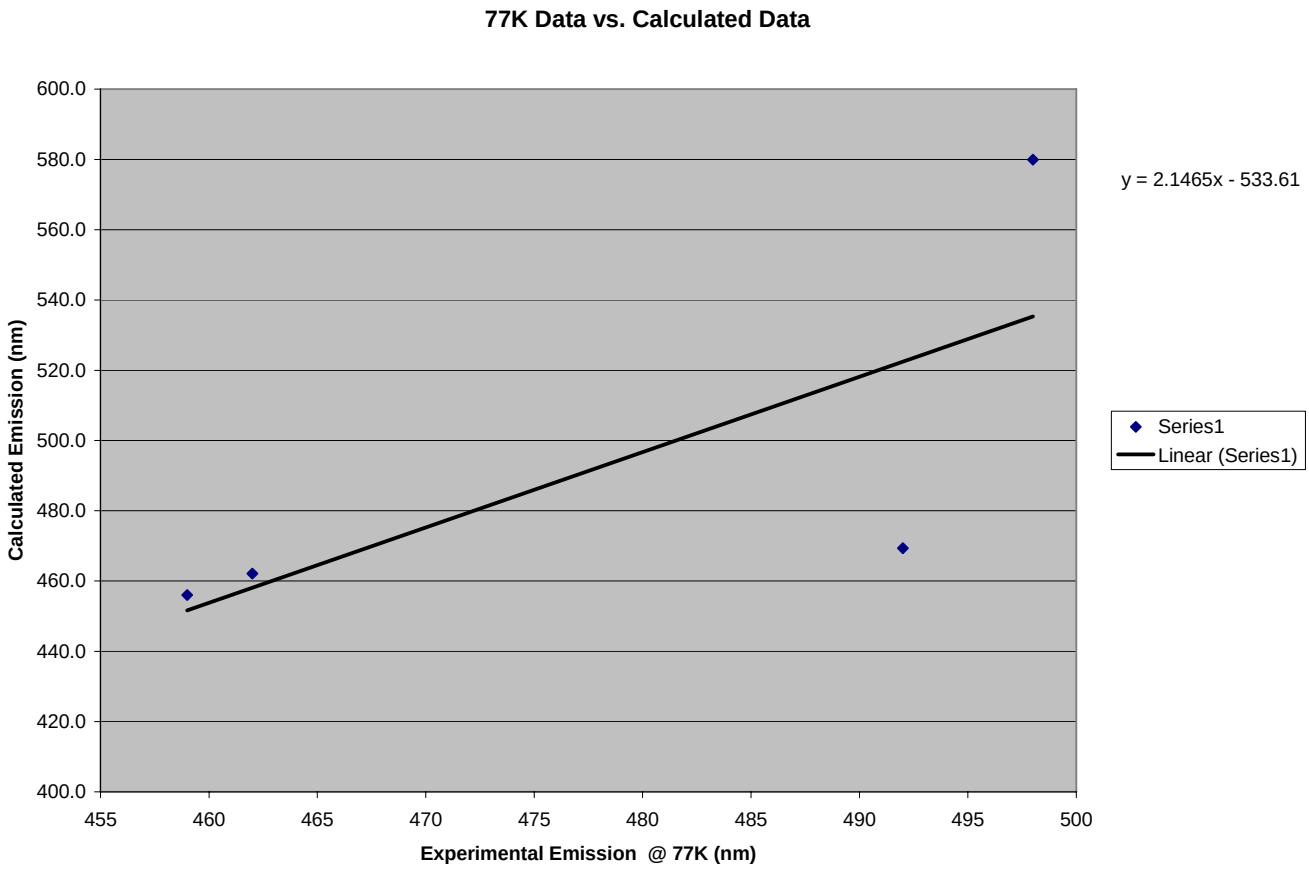

Figure 16: Linear correlation graph comparing the calculated data to emission maxima at 77K. This best-fit line gives the EFP

By using the linear equation y = 2.146x – 533.61 obtained from the correlation graph (Figure 16), the data in Table 6 were obtained. With this correction the average percent error was lowered from 5.46% to 2.60% and all compounds had more accurate wavelengths within approximately ± 25 nm. The highest deviation was with compound 1b being off by 24.7 nm.

Compound	Corrected Calculated Emission +EFP (nm)	Experimental Emission (nm) @ 77K	% Error
1a	461.1	459	0.45%
2a	463.9	462	0.41%
1b	467.3	492	5.03%
2b	519.1	498	4.23%

Table 6: Calculated vs. Experimental Emission Data @ 77K after incorporating the EFP to the calculated value.

Next, the 77K spectra maxima were plotted against the solution spectral data (Figure 9) to obtain a solvent correction factor. The equation of the best fitting line was y = x – 33.704, showing that this solvents correction would be a red-shift of 33.704 nm from the corrected 77K calculations. Table 7 shows the calculations after incorporating both the empirical fitting parameter and the solvent correction factor. Room temperature spectra maxima in a solution was predicted within ± 25 nm with an average percent error of 2.74%.

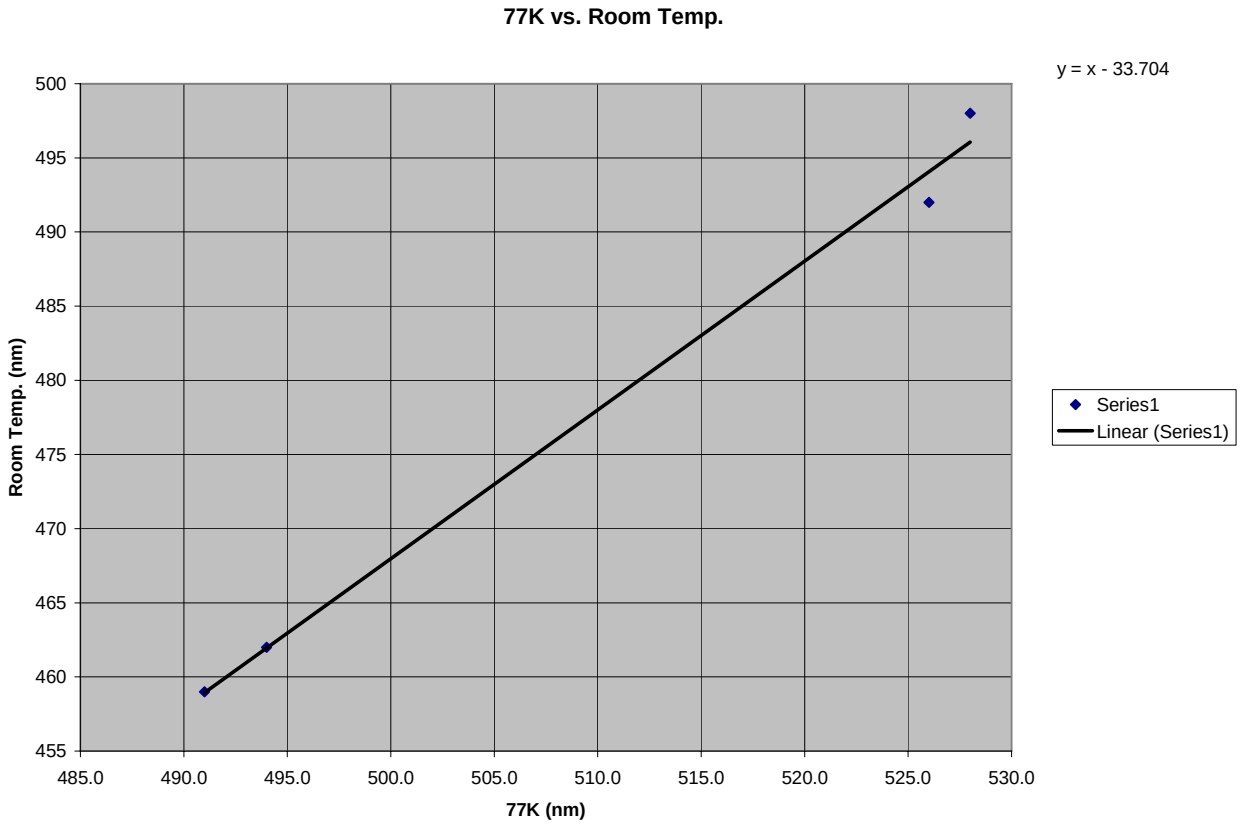

Figure 17: Linear correlation graph comparing the room temperature emission maxima to the emission maxima at 77K. This best-fit line gives the SCF

Compound	Corrected Calculated Emission + EFP & SCF (nm)	Experimental Emission (nm) Room Temp.	% Error
1a	494.8	491.0	0.77%
2a	497.6	494.0	0.73%
1b	501.0	526.0	4.76%
2b	552.8	528.0	4.70%

Table 7: Calculated vs. Experimental Emission Data @ 77K after incorporating the EFP or SCF to the calculated value.

It was not specified in the Rambacher paper[2] what solvent contained the molecules from which the spectra maxima was measured. However, because it is likely the same solvent was used, the data was compared with the calculated spectra maxima

with the EMP and SCF corrections. The results are shown in Table 8 with an average percent error of 5.84%. With the PIC's 1a, 2a, 1b, and 2b, there was an overall average percent error of 4.77%.

Compound	Corrected Calculated Emission + EFP & SCF (nm)	Experimental Emission (nm)	% Error
3a	525.9	573	8.20%
3b	573.7	571	0.37%
4b	564.7	626	9.74%
5b	537.5	540	0.37%
1e	506.3	550	8.00%
2e	510.9	550	7.09%
1f	510.9	550	7.09%

Figure 8: Calculated vs. Experimental Emission Data @ 77K after Incorporating the EFP and SCF to the Calculated Data

Chapter 3: Organic Synthesis of Two Theoretical PIC's

Introduction

As a test of our computational method, we synthesized two new compounds from our 4-amino-2-(2-pyridyl) quinoline in order to evaluate how the predicted fluorescence matched their actual emission. Calculations were performed on both compounds (Figure 4) and then we began synthesis of these compounds by converting the amino group into a diazonium salt by diazotization with nitrous acid (Figure 22). We then heated the reaction with the water, generating the phenol, or fluoride, giving the fluoride (see experimental).

Figure 18: Diazotization of an Amine

Experimental

Preparation of 4-hydroxy-2-(2-pyridyl) quinoline

A two neck 1 L round bottomed flask was fitted with a magnetic stirrer, a thermometer, and a pressure equalized dropping funnel. A flask was charged with 90 mL of concentrated HCl and 2.22 g (10 mmol) and 4-amino-2-(2-pyridyl) quinoline (2.20g, 10 mmol, 3a). The solution was cooled to 0 ºC in an ice bath. A pressure equalized dropping funnel was charged with 30 g (432 mmol) of sodium nitrite in 200 mL. With stirring, the solution of sodium nitrite was added drop-wise to the flask at a rate such that the temperature remained below 5 ºC. If added too quickly, the temperature would rise

and foaming would occur. During the addition the color of the solution changed from a bright yellow to a burnt orange. Following the addition of the sodium nitrite solution, stirring was continued for an additional 30 minutes at room temperature. At this point, the solution was a pale yellow. The solution was then heated slowly with the addition of 100 mL of water to convert the diazonium salt to the phenol. The solution was then neutralized and a white precipitate formed and was vacuum filtered. The compound 4-hydroxy-2-(2-pyridyl) quinoline (1.61 g) was recovered, ~73 % recovery.

Preparation of 4-fluoro-2-(2-pyridyl) quinoline

A two neck 1 L round bottomed flask was fitted with a magnetic stirrer, a thermometer, and a pressure equalized dropping funnel. 90 mL of concentrated HCl and 2.22 g (10 mmol) of 4-amino-2-(2-pyridyl) quinoline, 3a was added to the flask. The solution was cooled to 0 ºC in an ice bath. A pressure equalized dropping funnel was charged with 30 g (432 mmol) of sodium nitrite in 200 mL. With stirring, the solution of sodium nitrite was added drop wise to the flask at a rate such that the temperature remained below ~5 ºC. If added too quickly, the temperature would rise too quickly and would cause foaming to occur. During the addition the color of the solution changes from a bright yellow to a burnt orange. Following the addition of the sodium nitrite solution, stirring was continued for an additional 30 minutes at ~5 ºC while 100g of cesium fluoride in 100 mL of water was added to the solution. The solution was then slowly heated to approximately 75 ºC to induce the nucleophilic substitution of the diazonium salt with fluorine. A white crystalline solid immediately fell out of solution. The solution was allowed to cool and the solid vacuum filtered. 1.17 g of 4-fluoro-2-(2-

pyridyl) quinoline was recovered, ~52 % recovery. This prep was also attempted with the same amount of potassium fluoride instead of cesium fluoride with no product recovery. The higher reactivity of cesium fluoride is believed to have contributed to the success of this reaction.

Results

After being synthesized, both compounds were turned into PIC's by Dr. Morgan's patented technique. The 4-hydroxy-2-(2-pyridyl) quinoline PIC emission spectra showed three shoulders (Figure 19). To get the experimental emission, we weighted average of three points taken from approximately the middle of the shoulders giving a wavelength of 529 nm. The 4-fluoro-2-(2-pyridyl) quinoline PIC emission spectra showed one point at 508 nm (Figure 20). Both of these were within 25 nm of what our computation method from approach 1 and approach 2 had predicted as shown in Tables 5 and 6.

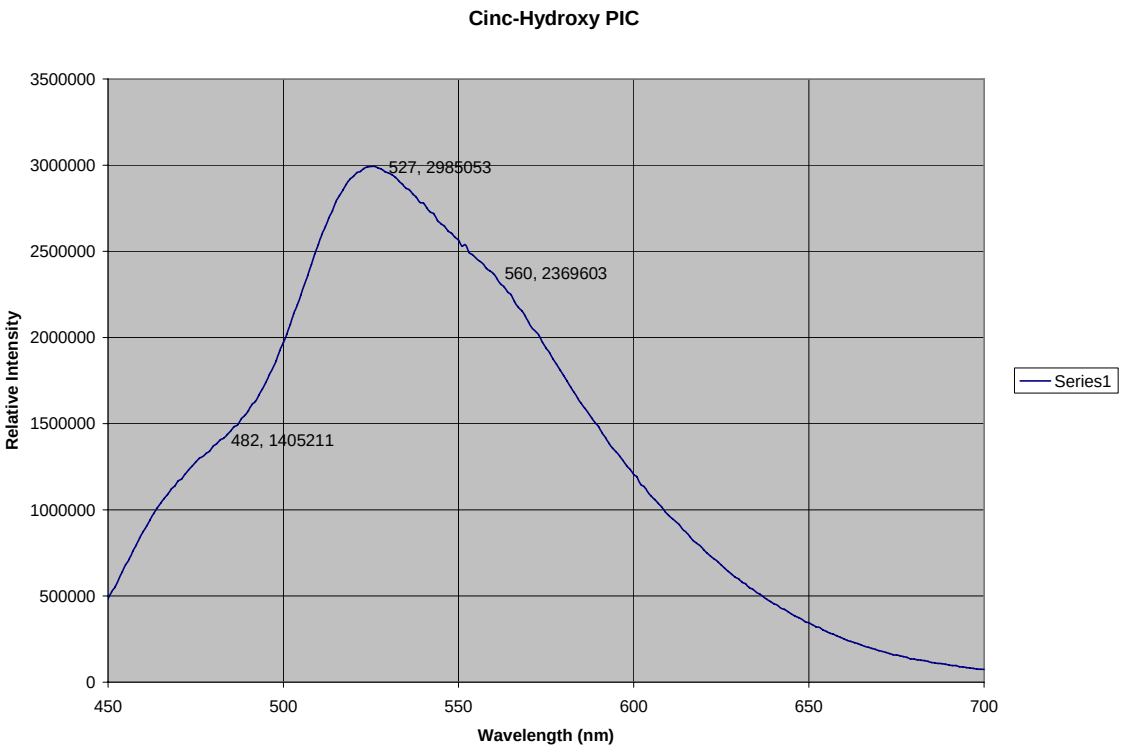

Figure 19: 4-hydroxy-2-(2-pyridyl) quinoline PIC Emission Spectra

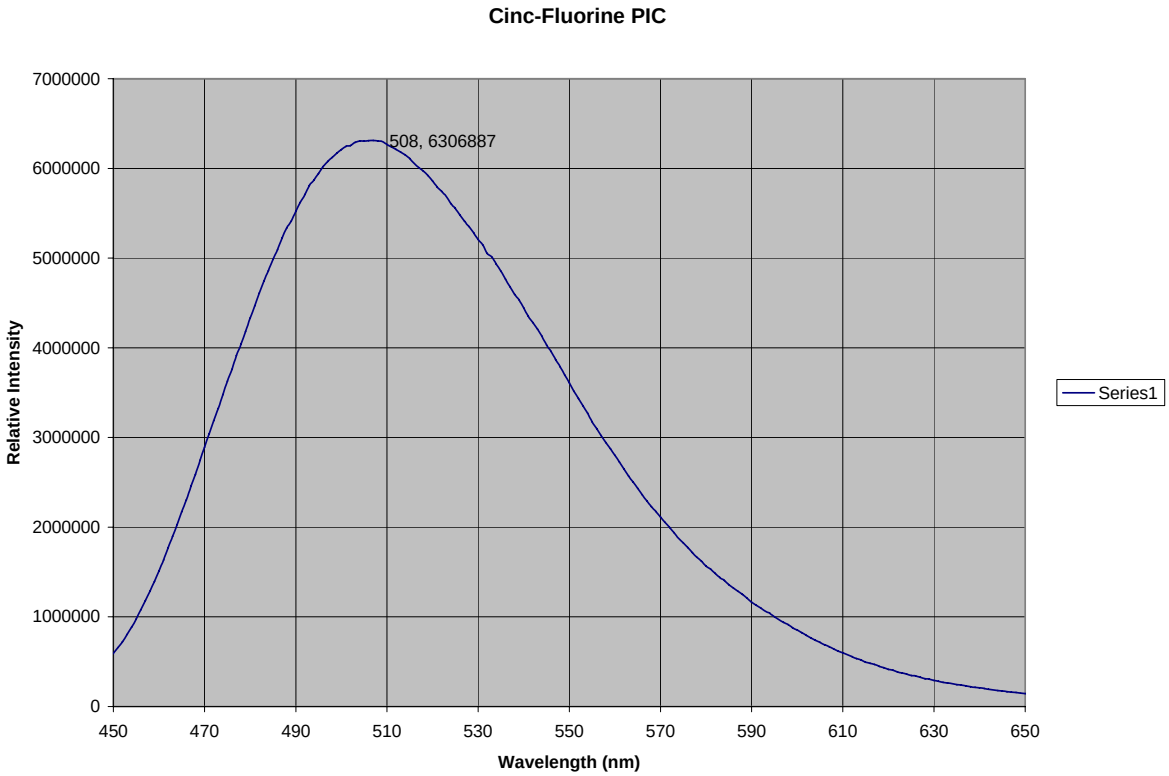

Figure 20: 4-fluoro-2-(2-pyridyl) quinoline PIC Emission Spectra

Compound	4-hydroxy-2-(2-pyridyl) quinoline PIC	4-fluoro-2-(2-pyridyl) quinoline PIC
Experimental Emission (nm)	529	508
Calculated Emission (nm)	552.6	537.3
% Error	4.5 %	5.8 %

Table 8: Experimental vs. Calculated Emission Spectra of two new synthesized PIC's from Approach #1

Compound	4-hydroxy-2-(2-pyridyl) quinoline PIC	4-fluoro-2-(2-pyridyl) quinoline PIC
Experimental Emission (nm)	529	508
Calculated Emission (nm)	551.3	535.4
% Error	4.2 %	5.39 %

Table 9: Experimental vs. Calculated Emission Spectra of two new synthesized PIC's from Approach #2

Chapter 4: Summary and Conclusion

With this computational method of predicting fluorescence, the expense of countless hours in the lab and chemicals synthesizing compounds that do not have the intended fluorescent properties can be diminished. This should help to not only focus on those fluorescent dyes that the market demands, but also lead to a better understanding that the effects of functional groups, solvation, size of molecules, and other factors have on the fluorescence of a molecule. In the age of computers, finding a safe, easy way to do chemical research is welcomed and soon with perfection will save countless amounts of wasted chemicals and time.

Based originally on Fabian's work,[3-5] the abilities of computational chemistry have been expanded to not only predict the fluorescence of more complex molecules, but also predict them within hours, instead of days or weeks. The future holds an expanded study of the several aspects that can influence fluorescence, therefore gaining a greater understanding of fluorescence itself.

Two approaches were taken to include a correction factor into the equation to allow for more accurate predictions. The first was a direct correlation between the calculated data and the experimental finding an empirical fitting parameter and was accurate within ~25 nm of the actual spectra maxima. For now, this seems to be an acceptable, quick method for predicting the fluorescence spectra of the PIC's developed by Dr. Morgan's group.

As seen from the spectra, this computational method from both approaches predicted within 25nm of the actual emission spectra. Several things can contribute to the error shown in Table 5 such as the purity and concentration of the samples and

solvent effects with the different functional groups and the molecules themselves. These reasons are why we needed a correlation graph to incorporate a "fudge factor" when predicting fluorescence. However, we were pleased with the ability to predict fluorescence within 25 nm of the actual emission. With this ability, we can at least predict the region of the visible spectrum that a potential fluorescent dye will emit.

Although there was little data to support the second approach, it is believed that it can be a much better prediction method upon further research. The four fluorescence spectra of the 1a, 2a, 1b, and 2b PIC's were the only data available and therefore did not provide enough data to provide a proper argument. However, it was found that with the greater the increase in dipole moment from the ground to the excited state, the more deviation of the predictions from the actual 77K emission spectra. It is believed that the key to finding an extremely accurate way of predicting fluorescence spectra maxima is to find a correlation between the dipole change of electric states and the solvent they are in. For example, the greatest deviation before any incorporation of the EMP or SCF from our data was PIC 2b with a percent error of 16.59% which is four times the percent error of the next highest deviation. PIC 2b also had an increase of ~7 debye, which was seven times that of the next highest deviation. This is caused buy the methanol/ethanol non-polar solvent effects destabilizing the excited state and stabilizing the ground state (even in a crystal matrix) causing the predicted in vacuo calculation to be much higher than the experimental value obtained in a non-polar solvent. With further studies on the fluorescence spectra maxima at 77K versus the dipole moment change between excited states, solvent effects will be better understood leading to more accurate predictions utilizing computational chemistry.

References

1) Donovan R. J. and Morgan R. J.; U.S. Patent 5,874,587 Feb. 23, 1999
2) Rambacher R. W.; *Pyridoimidazolium Cationic Dyes: Theory, Synthesis, and Sub-cellular Localization*; http://www.marshall.edu/etd/descript.asp?ref=163 (accessed 4/20/03)
3) Fabian W. M. F.; *Journal of Molecular Structure.* **1999** *477* 209-220
4) Fabian W. M. F., Niederreiter K.S., Uray G. and Stadlbauer W.; *Journal of Molecular Structure;* 477 (1999) 209-220
5) Zerner M.C., Reidlinger C., Fabian W.M.F. and Junek H.; *Journal of Molecular Structure;* (Theochem) 543 (2001) 129-146
6) Haugland, Richard P.; *Handbook of Fluorescent Probes and Research Products: Ninth Edition;* Molecular Probes Inc.; 2002
7) Clark, Tim; *A Handbook of Computational Chemistry;* John Wiley and Sons; 1985
8) Edwards W.D., Weiner B. and Zerner M.C.; *J. Am. Chem. Soc.*; **1986** *108* 2196
9) Wasielewska E., Witko M., Stochel G. and Stasicka Z., *Chemistry –AEuropean Journal*; **1997** *3* 609
10) Edwards W.D., Weiner B. and Zerner M.C.; *J. Phys. Chem.*; **1988** *92* 6188
11) Anderson W.P., Edwards W.D. and Zerner M.C.; *Inorg. Chem.*; **1986** *25* 2728
12) Loew G.H., Herman Z.S. and Zerner M.C.; *Int. J. Quantum Chem.*; **1988** *33* 177
13) Anderson W.P., Edwards W.D., Zerner M.C. and Canuto S.; *Chem. Phys. Lett.*; **1982** *88* 185
14) Stavrev K.K. and Zerner M.C.; *Chem. Europ. J.*; **1996** *2* 34
15) McQuarrie D.A. and Simon J.D.; *Physical Chemistry: A Molecular Approach;* University Science Books; 1997
16) Son, Jae Keun, Kim, Seung, III, Jahng, Yumgdong; *Heterocycles;* (2001), 55 (10), 1981-1986

Appendix A: Fluorescence Prediction with Hyperchem (Step by Step)

Structure Drawing

Using Hyperchem 7.5 is a fairly easy process. To avoid any complications with translation of structure, the structure was drawn in the program itself instead of importing a structure from another graphics program as was done in the Rambacher paper.[2] Before drawing the structure, the "Explicit Hydrogens" option was checked under the "Build" menu (Figure 21). Next, the rendering settings under the "Display" menu and selected the atoms and bonds to be shown as "Balls and Cylinders" carbon as the default element by going to "Default Element" option under the "Build" menu (Figure 21). Here is where the element selections were chosen throughout the drawing process (Figure 23).

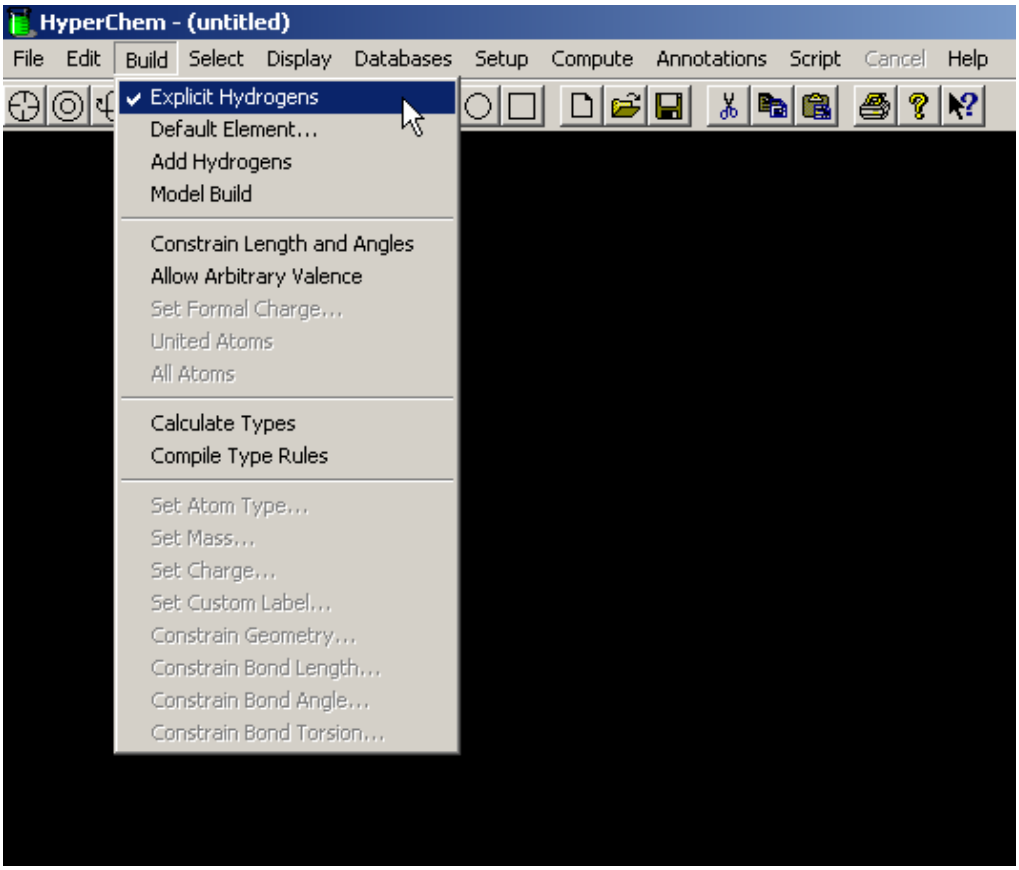

Figure21: Explicit Hydrogens option under the Build menu

Using the drawing tool (Figure 22), the basic structure was drawn without multiple bonds using carbon atoms (Figure 24). The carbon atoms were replaced with the other necessary atoms (Figure 25) using the “Default Element” tool (Figure 23). After the structure was completed, the “Model Build” option under the “Build” menu was selected (Figure 26).

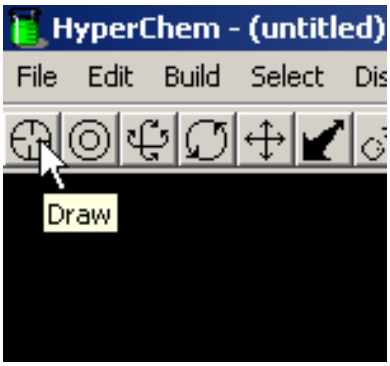

Figure 22: Drawing Tool

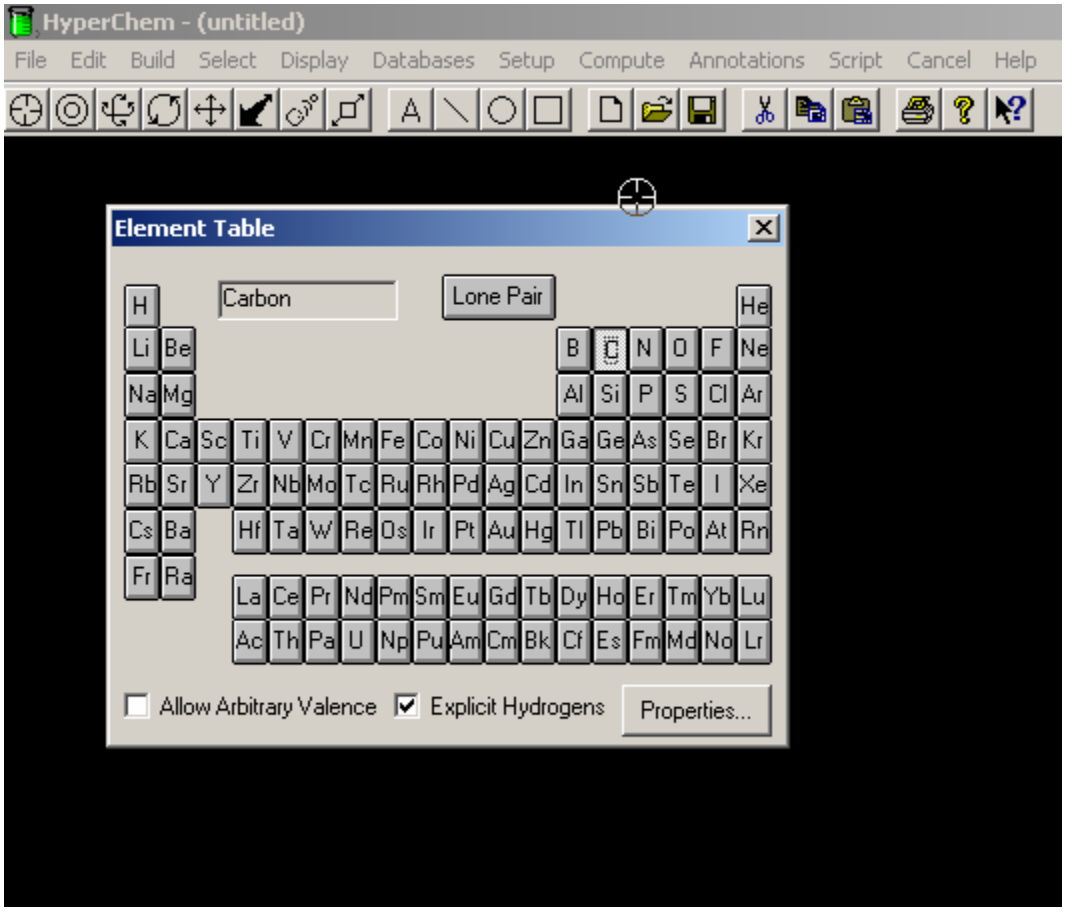

Figure 23: Default Element Selection Table

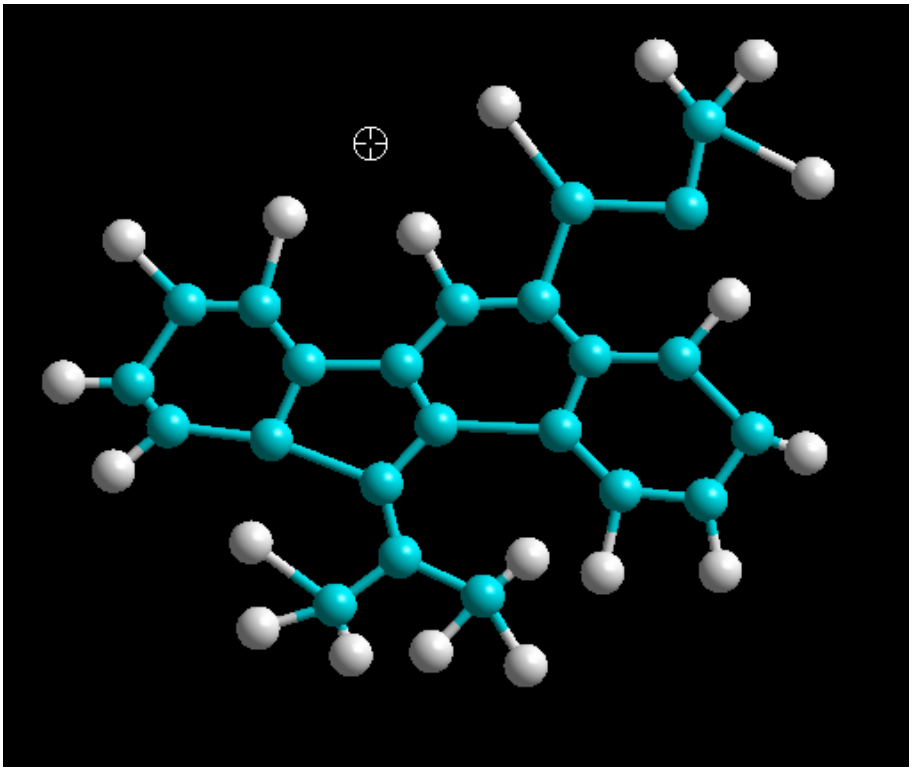

Figure 24: Basic structure containing all carbon atoms. In Hyperchem, the elements are assumed to be Hydrogens until another bond is attached.

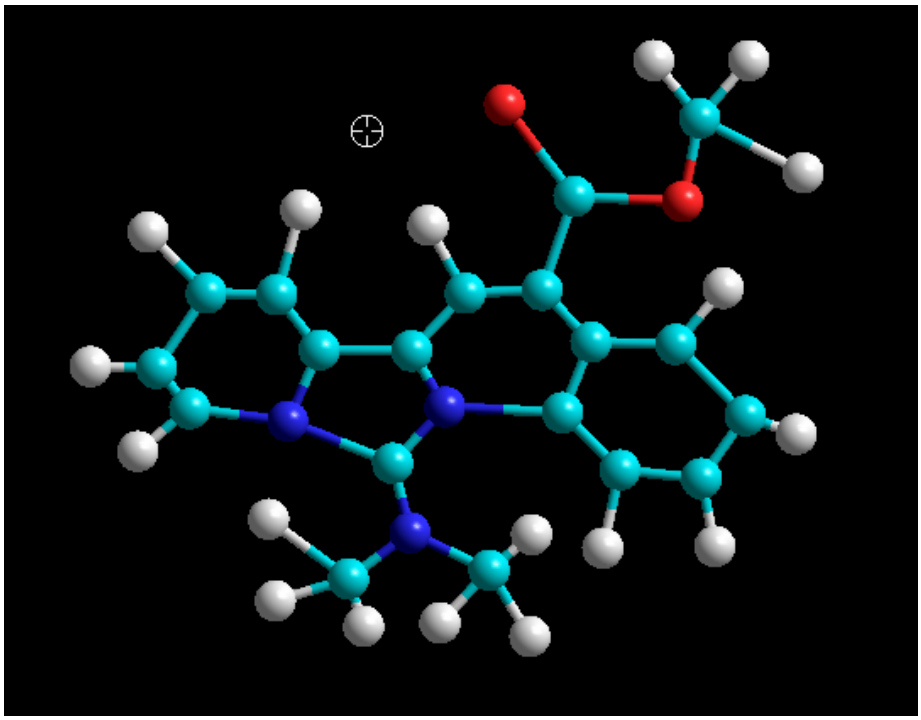

Figure 25: Completed structure with correct elements.

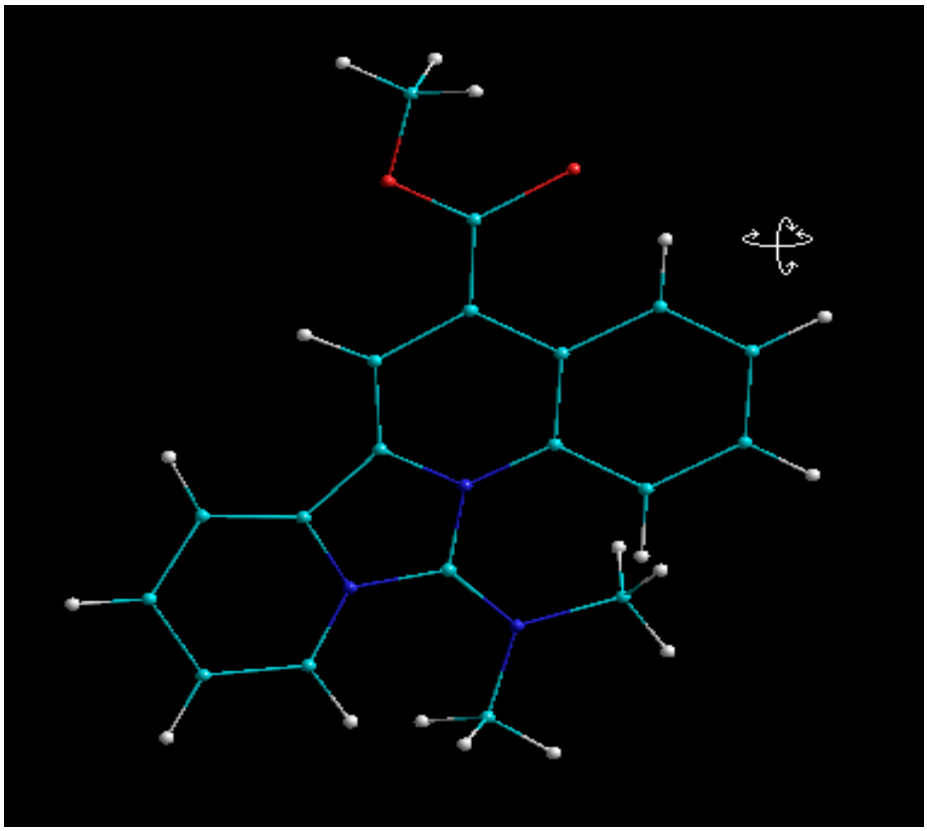

Figure 26: Molecule that has been completely drawn and built.

Calculations of the Ground State

With the desired molecule drawn and built, calculations were run on the structure in its excited state. Next, the desired parameters were set by selecting the "Semi-Empirical" option in the "Setup" menu (Figure 27) which brings up the list of method options (Figure 28). For the ground state, the Fabian work was followed by running the geometric optimization under AM1 conditions.[3-5] After selecting AM1, the parameters were set by clicking the "Option" button found on the "Semi-Empirical" list (Figure 28). In this window the only thing changed was the "Charge" and "Spin Multiplicity" were set to 1 (Figure 29). Under the "Configuration Interaction" button on the "Options" window the "CI Method" was set to "None" (Figure 30).

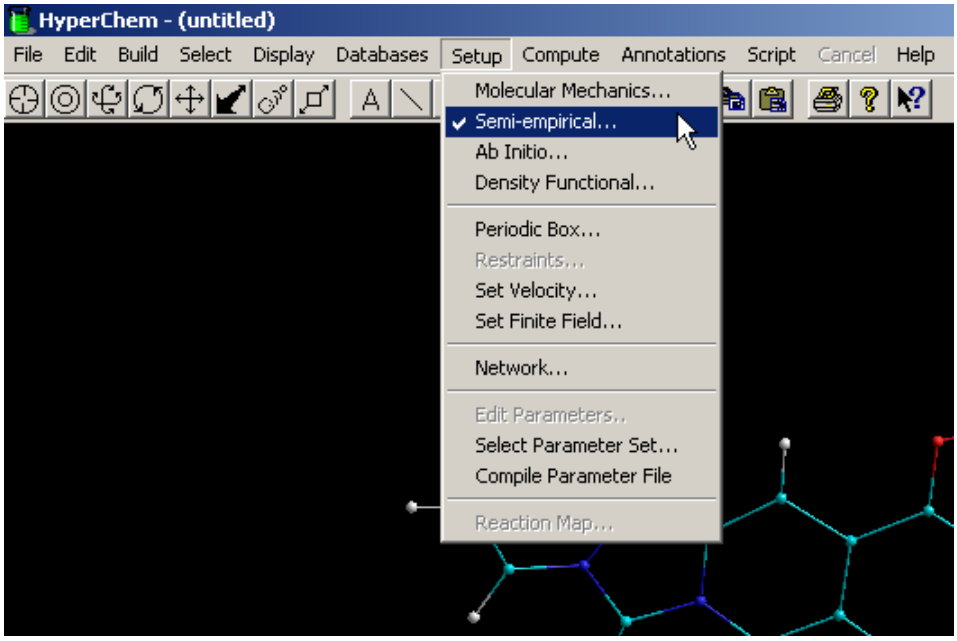

Figure 27: The "Setup" menu.

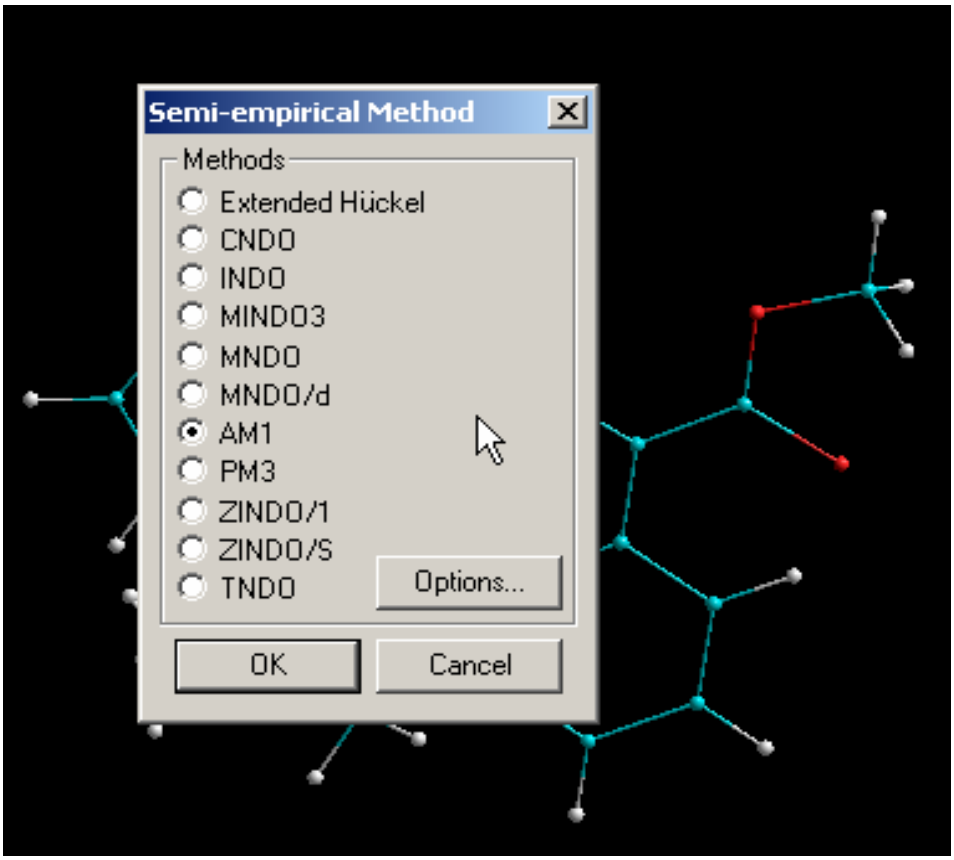

Figure 28: Semi-Empirical Method List

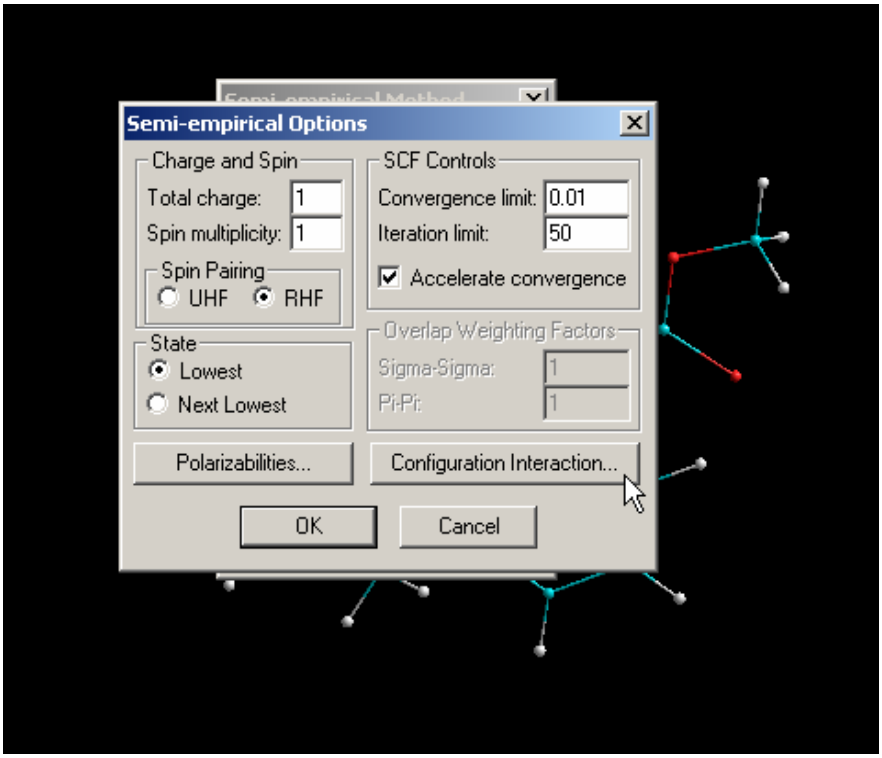

Figure 29: Semi-Empirical Options

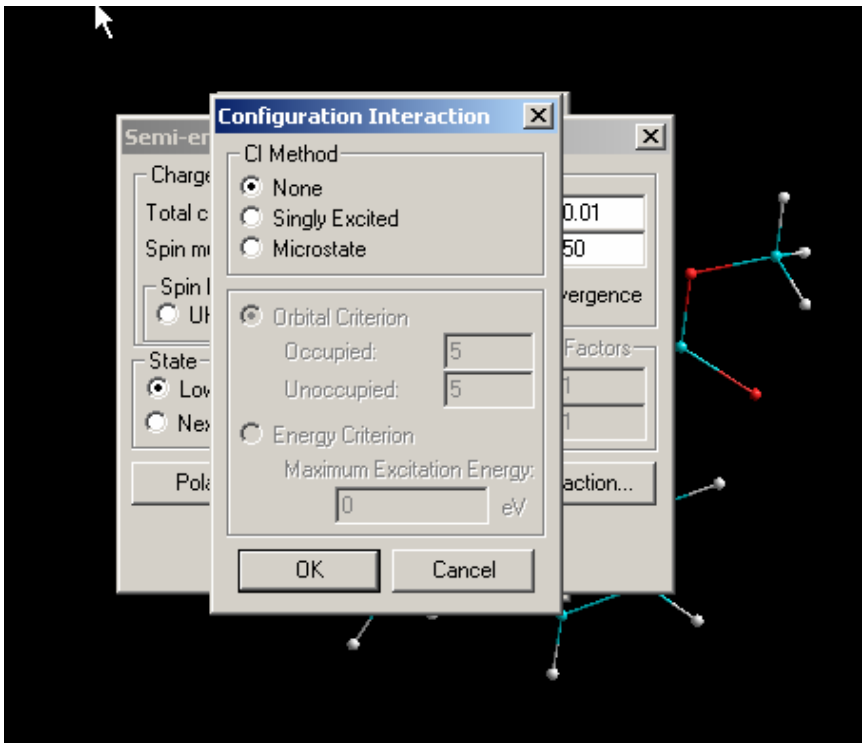

Figure 30: Configuration Interaction Options for the AM1 geometric optimization of the ground state

After setting the parameters, the “Geometric Optimization” was selected under the “Compute” menu (Figure 31). Here, “Polak-Ribiere” was selected (Figure 32). Also, in this window, the RMS gradient was changed to 0.01 for accuracy and the cycles were set to 1000 to allow for a complete optimization.

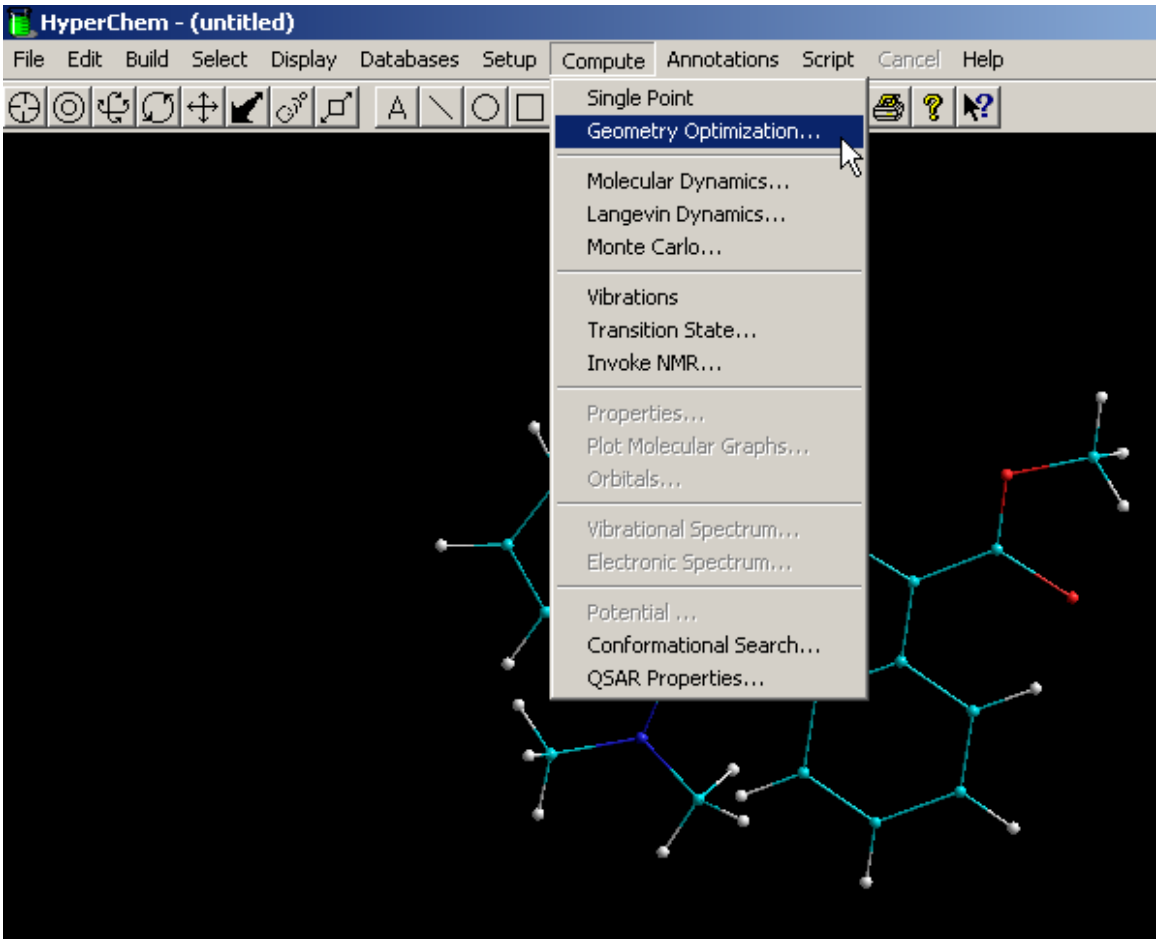

Figure 31: The “Compute” Menu.

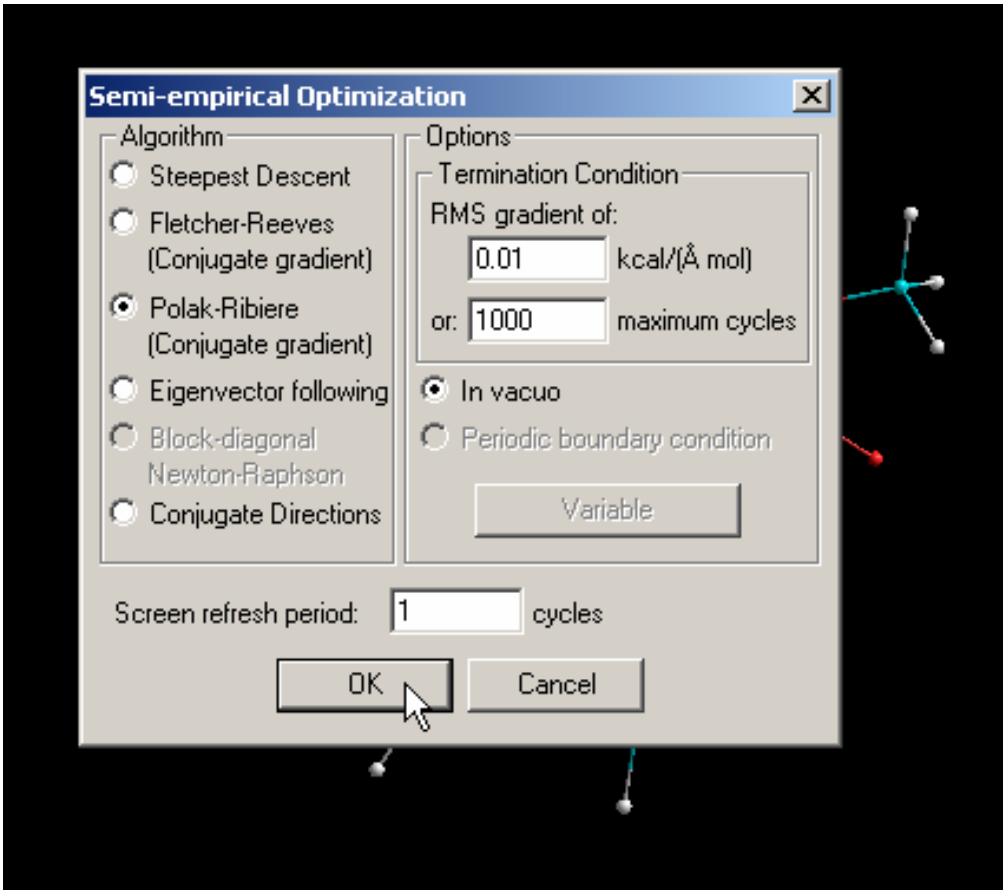

Figure 32: Geometric Optimization Options.

After the geometric optimization was complete, a log file was started to record the calculations by going to the "File" menu and selecting "Start Log" (Figure 29). After starting a log, ZINDO/S was selected under the "Semi-empirical" list (Figure 28). Under the Configuration Interaction window "Singly Excited" and "Orbital Criterion" were selected the Occupied and Unoccupied orbitals were set to 5 (Figure 34). "Single Point" under the "Compute" menu was then selected to calculate the total energy and charge and electron distribution. Next, the electronic spectrum of the ground state was calculated to identify the absorption spectrum. Finally, under the "File" menu "Stop Log" was selected.

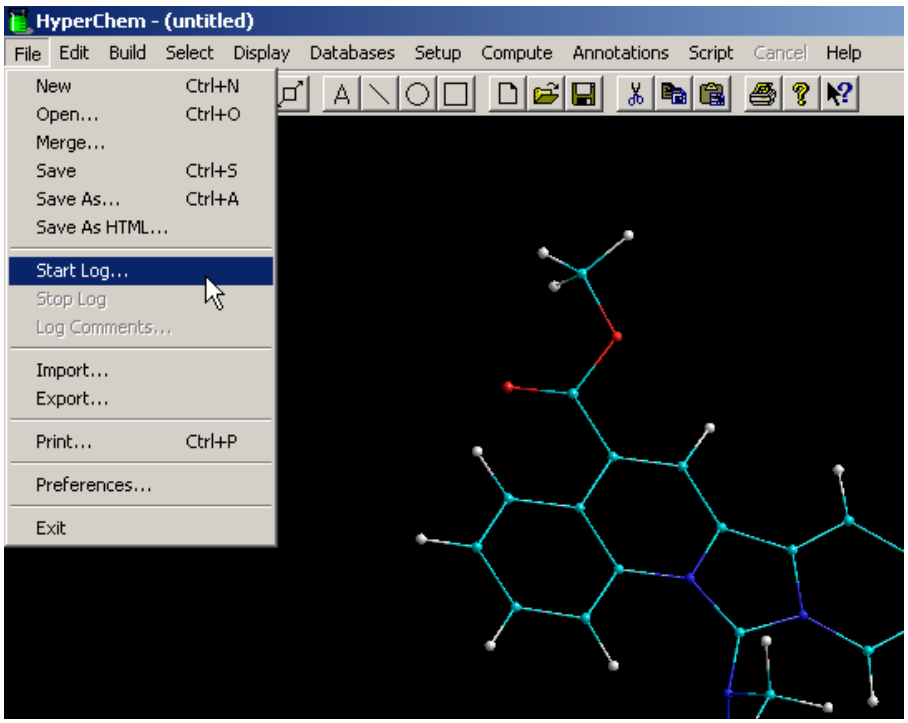

Figure 33: File Menu

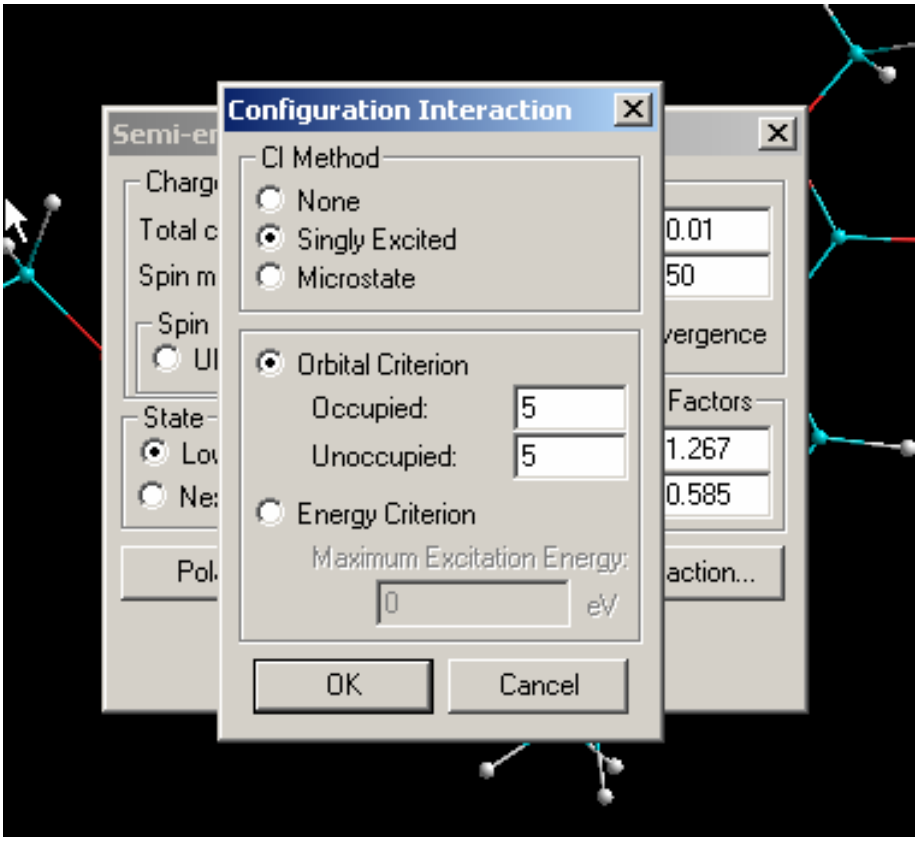

Figure 34: Configuration Interaction Options

Calculations at the Singly Excited State

After the ground-state simulation, calculations were performed on the structure after it had been singly excited. To begin, the desired parameters were set by selecting ZINDO/1 as the method (Figure 28). The optimization was then run at the excited state to simulate internal conversion. The only method available in Hyperchem for excited geometric optimization is "Conjugate Directions" (Figure 35).

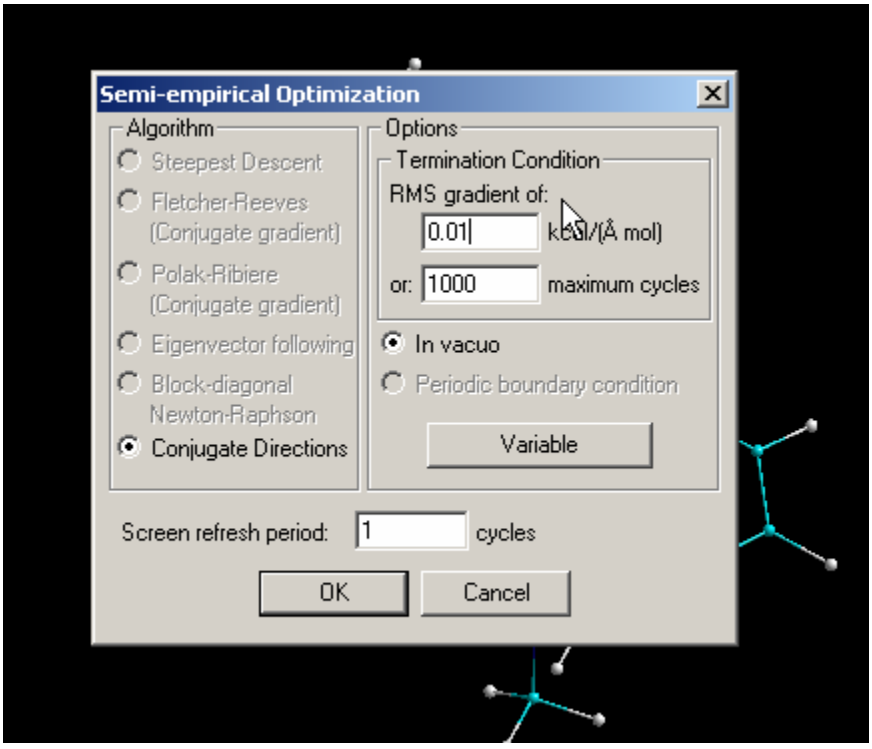

Figure 35: Excited State Geometric Optimization Options

After the optimization was complete, ZINDO/S was selected as the semi-empirical method the single point calculation was run on the ground state. A new log was then started to capture the calculations of the excited state. As before, a single point

calculation was performed generating an electronic spectrum, showing the theoretical emission spectrum and the log was then stopped.

Appendix B: Example of a Hyperchem Log File

```
HyperChem log start -- Tue Nov 02 19:41:56 2004.
Single Point, SemiEmpirical, molecule = C:\Documents and Settings\Craig Lathey\My Documents\Research\Cinc-CarboxAcid\AM1 Ground GO.hin.
ZINDOS
Convergence limit = 0.0100000  Iteration limit = 50
Overlap weighting factors: P(Sigma-Sigma) = 1.2670 and P(Pi-Pi) = 0.5850
Accelerate convergence = YES
RHF Calculation:

Singlet state calculation
Configuration interaction will be used
Number of electrons = 114
Number of Double Occupied Levels = 57
Charge on the System = 1
Total Orbitals = 108
Number of Occupied Orbitals Used in CI = 5
Number of Unoccupied Orbitals Used in CI = 5
Starting ZINDO/S calculation with 108 orbitals
Iteration = 1 Difference = 66149.76412
Iteration = 2 Difference = 375.59255
Iteration = 3 Difference = 33.69926
Iteration = 4 Difference = 6.06397
Iteration = 5 Difference = 8.45631
Iteration = 6 Difference = 0.33825
Iteration = 7 Difference = 0.12762
Iteration = 8 Difference = 0.01820
Iteration = 9 Difference = 0.00872
Starting a singly excited CI calculation with 51 configurations.
Computing the integrals for CI matrix: done 0%.
Computing the integrals for CI matrix: done 10%.
Computing the integrals for CI matrix: done 20%.
Computing the integrals for CI matrix: done 30%.
Computing the integrals for CI matrix: done 40%.
Computing the integrals for CI matrix: done 50%.
Computing the integrals for CI matrix: done 60%.
Computing the integrals for CI matrix: done 70%.
Computing the integrals for CI matrix: done 80%.
Computing the integrals for CI matrix: done 90%.
Computing the integrals for CI matrix: done 100%.
Computing the CI matrix...
Diagonalizing the CI matrix...
Computing the properties of the CI states...

             ***********************************
             ********** UV Spectrum **********
             ***********************************

 ---- Absolute Energy in eV.
 ---- Dipole Moments in Debye.


********************************************************************************


  0 (Reference)  Absolute Energy     -4414.06738

        1     Spin S                0.00
              State Dipole          10.3372

              State Dipole Components         1.0329  -10.2817   -0.2777


  1 (Transition) Excitation Energy        1198.5 nm
                                  8344.0 1/cm

      1 ->   2  Spin S                1.00
              State Dipole          12.3169
              Oscillator Strength     0.0000

              State Dipole Components         1.2937  -12.2480   -0.1299
              Transition Dipole Components   -0.0000   -0.0000    0.0000

     Spin Up :  Occ. MO  -->  Unocc. MO  Coefficients
     ---------------------------------------------------
                57  -->    58           0.670086

     Spin Down:  Occ. MO  -->  Unocc. MO  Coefficients
     ---------------------------------------------------
                57  -->    58           0.670086


  2 (Transition) Excitation Energy         913.8 nm
                                 10943.8 1/cm

      1 ->   3  Spin S                1.00
              State Dipole           5.8742
              Oscillator Strength     0.0000

              State Dipole Components         1.8446   -5.5555   -0.4899
              Transition Dipole Components    0.0000   -0.0000    0.0000
```

Spin Up : Occ. MO --> Unocc. MO Coefficients
---
57 --> 59 -0.650198

Spin Down: Occ. MO --> Unocc. MO Coefficients
---
57 --> 59 -0.650198

3 (Transition) Excitation Energy 524.1 nm
19080.3 1/cm

1 -> 4 Spin S 1.00
State Dipole 8.3524
Oscillator Strength 0.0000

State Dipole Components -2.4216 -7.9657 -0.6677
Transition Dipole Components -0.0000 0.0000 -0.0000

Spin Up : Occ. MO --> Unocc. MO Coefficients
---
57 --> 60 -0.599024

Spin Down: Occ. MO --> Unocc. MO Coefficients
---
57 --> 60 -0.599024

4 (Transition) Excitation Energy 469.9 nm
21279.7 1/cm

1 -> 5 Spin S -0.00
State Dipole 10.2356
Oscillator Strength 0.9268

State Dipole Components -1.1163 -10.1648 -0.4454
Transition Dipole Components -1.1206 9.5387 -0.6175

Spin Up : Occ. MO --> Unocc. MO Coefficients
---
57 --> 58 0.692391

Spin Down: Occ. MO --> Unocc. MO Coefficients
---
57 --> 58 -0.692391

5 (Transition) Excitation Energy 407.9 nm
24517.1 1/cm

1 -> 6 Spin S -0.00
State Dipole 7.5472
Oscillator Strength 0.2668

State Dipole Components 1.4834 -7.3891 -0.4020
Transition Dipole Components 4.2100 -2.2973 0.3696

Spin Up : Occ. MO --> Unocc. MO Coefficients
---
57 --> 59 0.637567

Spin Down: Occ. MO --> Unocc. MO Coefficients
---
57 --> 59 -0.637567

6 (Transition) Excitation Energy 378.4 nm
26427.8 1/cm

1 -> 7 Spin S 1.00
State Dipole 7.2150
Oscillator Strength 0.0000

State Dipole Components -5.5418 -4.4944 -1.0696
Transition Dipole Components -0.0000 0.0000 -0.0000

Spin Up : Occ. MO --> Unocc. MO Coefficients
---
56 --> 58 -0.616965

Spin Down: Occ. MO --> Unocc. MO Coefficients
---
56 --> 58 -0.616965

7 (Transition) Excitation Energy 371.8 nm
26897.1 1/cm

1 -> 8 Spin S 1.00
State Dipole 11.8949
Oscillator Strength 0.0000

State Dipole Components 0.5577 -11.8807 -0.1563
Transition Dipole Components 0.0000 -0.0000 0.0000

Spin Up : Occ. MO --> Unocc. MO Coefficients
---
57 --> 61 -0.501799

Spin Down: Occ. MO --> Unocc. MO Coefficients
---
57 --> 61 -0.501799

8 (Transition) Excitation Energy 353.1 nm
28321.4 1/cm

1 -> 9 Spin S 1.00
State Dipole 2.7537
Oscillator Strength 0.0000

State Dipole Components -0.2321 -2.7413 0.1211
Transition Dipole Components 0.0000 0.0000 -0.0000

Spin Up : Occ. MO --> Unocc. MO Coefficients
---
55 --> 58 -0.371939
54 --> 58 0.410333

Spin Down: Occ. MO --> Unocc. MO Coefficients
---
55 --> 58 -0.371939
54 --> 58 0.410333

9 (Transition) Excitation Energy 342.7 nm
29183.4 1/cm

1 -> 10 Spin S 1.00
State Dipole 6.5328
Oscillator Strength 0.0000

State Dipole Components -0.4376 -6.5166 -0.1390
Transition Dipole Components -0.0000 0.0000 -0.0000

Spin Up : Occ. MO --> Unocc. MO Coefficients
---
55 --> 58 -0.421382
54 --> 58 -0.356038

Spin Down: Occ. MO --> Unocc. MO Coefficients
---
55 --> 58 -0.421382
54 --> 58 -0.356038

10 (Transition) Excitation Energy 342.0 nm
29240.5 1/cm

1 -> 11 Spin S 0.00
State Dipole 6.7490
Oscillator Strength 0.0080

State Dipole Components -1.5784 -6.5231 -0.7114
Transition Dipole Components -0.7485 0.0579 -0.1384

Spin Up : Occ. MO --> Unocc. MO Coefficients
---
57 --> 60 -0.661132

Spin Down: Occ. MO --> Unocc. MO Coefficients
---
57 --> 60 0.661132

11 (Transition) Excitation Energy 331.3 nm
30179.8 1/cm

1 -> 12 Spin S -0.00
State Dipole 0.8604
Oscillator Strength 0.0037

State Dipole Components -0.6370 0.5249 0.2427
Transition Dipole Components -0.0682 0.5093 0.0068

Spin Up : Occ. MO --> Unocc. MO Coefficients
---
54 --> 58 0.497262

Spin Down: Occ. MO --> Unocc. MO Coefficients
---
54 --> 58 -0.497262

12 (Transition) Excitation Energy 316.3 nm

31617.9 1/cm

1 -> 13 Spin S 1.00
State Dipole 5.7712
Oscillator Strength 0.0000

State Dipole Components -3.4721 -4.5183 -0.9142
Transition Dipole Components -0.0000 0.0000 -0.0000

Spin Up : Occ. MO --> Unocc. MO Coefficients
---
56 --> 59 -0.525405
56 --> 61 0.397097

Spin Down: Occ. MO --> Unocc. MO Coefficients
---
56 --> 59 -0.525405
56 --> 61 0.397097

13 (Transition) Excitation Energy 315.6 nm
31681.3 1/cm

1 -> 14 Spin S 0.00
State Dipole 7.5759
Oscillator Strength 0.1947

State Dipole Components -6.4699 -3.7978 -1.0542
Transition Dipole Components -3.0422 1.9191 -0.3625

Spin Up : Occ. MO --> Unocc. MO Coefficients
---
56 --> 58 -0.569906

Spin Down: Occ. MO --> Unocc. MO Coefficients
---
56 --> 58 0.569906

14 (Transition) Excitation Energy 302.5 nm
33054.2 1/cm

1 -> 15 Spin S 1.00
State Dipole 17.5968
Oscillator Strength 0.0000

State Dipole Components -0.4333 -17.5914 0.0231
Transition Dipole Components 0.0000 -0.0000 0.0000

Spin Up : Occ. MO --> Unocc. MO Coefficients
---
57 --> 62 -0.611367

Spin Down: Occ. MO --> Unocc. MO Coefficients
---
57 --> 62 -0.611367

15 (Transition) Excitation Energy 301.3 nm
33185.4 1/cm

1 -> 16 Spin S 0.00
State Dipole 8.4245
Oscillator Strength 0.2399

State Dipole Components -0.1574 -8.4094 -0.4784
Transition Dipole Components 3.5527 -1.6294 0.3127

Spin Up : Occ. MO --> Unocc. MO Coefficients
---
57 --> 61 0.335264
55 --> 58 -0.478092

Spin Down: Occ. MO --> Unocc. MO Coefficients
---
57 --> 61 -0.335264
55 --> 58 0.478092

16 (Transition) Excitation Energy 285.5 nm
35031.9 1/cm

1 -> 17 Spin S 1.00
State Dipole 15.9301
Oscillator Strength 0.0000

State Dipole Components -7.7078 -13.9326 -0.4904
Transition Dipole Components 0.0000 -0.0000 -0.0000

Spin Up : Occ. MO --> Unocc. MO Coefficients
---
53 --> 58 -0.341487
53 --> 59 -0.592441

Spin Down: Occ. MO --> Unocc. MO Coefficients
---
53 --> 58 -0.341487
53 --> 59 -0.592441

17 (Transition) Excitation Energy 283.1 nm
35324.5 1/cm

1 -> 18 Spin S 0.00
State Dipole 16.0332
Oscillator Strength 0.0044

State Dipole Components -7.7712 -14.0155 -0.4877
Transition Dipole Components 0.0903 -0.4397 -0.2557

Spin Up : Occ. MO --> Unocc. MO Coefficients
---
53 --> 58 -0.348351
53 --> 59 -0.590388

Spin Down: Occ. MO --> Unocc. MO Coefficients
---
53 --> 58 0.348351
53 --> 59 0.590388

18 (Transition) Excitation Energy 278.0 nm
35969.6 1/cm

1 -> 19 Spin S 1.00
State Dipole 4.9083
Oscillator Strength 0.0000

State Dipole Components -0.0093 -4.8569 -0.7089
Transition Dipole Components 0.0000 0.0000 0.0000

Spin Up : Occ. MO --> Unocc. MO Coefficients
---
55 --> 59 0.603280

Spin Down: Occ. MO --> Unocc. MO Coefficients
---
55 --> 59 0.603280

19 (Transition) Excitation Energy 274.0 nm
36500.8 1/cm

1 -> 20 Spin S 0.00
State Dipole 14.1185
Oscillator Strength 0.3715

State Dipole Components 2.0733 -13.9653 0.0486
Transition Dipole Components 4.5622 0.8792 0.2448

Spin Up : Occ. MO --> Unocc. MO Coefficients
---
57 --> 61 -0.499755
55 --> 58 -0.388249

Spin Down: Occ. MO --> Unocc. MO Coefficients
---
57 --> 61 0.499755
55 --> 58 0.388249

20 (Transition) Excitation Energy 266.5 nm
37520.7 1/cm

1 -> 21 Spin S 0.00
State Dipole 16.6593
Oscillator Strength 0.0701

State Dipole Components -0.2357 -16.6576 0.0347
Transition Dipole Components -0.9481 -1.7525 -0.0224

Spin Up : Occ. MO --> Unocc. MO Coefficients
---
57 --> 62 -0.496656
56 --> 59 0.322409

Spin Down: Occ. MO --> Unocc. MO Coefficients
---
57 --> 62 0.496656
56 --> 59 -0.322409

21 (Transition) Excitation Energy 261.8 nm
38200.2 1/cm

1 -> 22 Spin S -0.00

State Dipole 3.3854
Oscillator Strength 0.5750

State Dipole Components -3.1493 0.0722 -1.2401
Transition Dipole Components -0.1399 5.6432 -0.3799

Spin Up : Occ. MO --> Unocc. MO Coefficients
---
56 --> 59 -0.348622
55 --> 59 0.552306

Spin Down: Occ. MO --> Unocc. MO Coefficients
---
56 --> 59 0.348622
55 --> 59 -0.552306

22 (Transition) Excitation Energy 254.3 nm
39320.4 1/cm

1 -> 23 Spin S 0.00
State Dipole 5.9465
Oscillator Strength 0.2409

State Dipole Components -2.6691 -5.2430 -0.8642
Transition Dipole Components 2.7911 -2.2591 0.3702

Spin Up : Occ. MO --> Unocc. MO Coefficients
---
57 --> 62 0.408055
56 --> 59 0.446214

Spin Down: Occ. MO --> Unocc. MO Coefficients
---
57 --> 62 -0.408055
56 --> 59 -0.446214

23 (Transition) Excitation Energy 249.0 nm
40166.2 1/cm

1 -> 24 Spin S 1.00
State Dipole 5.8417
Oscillator Strength 0.0000

State Dipole Components -4.0443 -4.0932 -1.0074
Transition Dipole Components -0.0000 -0.0000 -0.0000

Spin Up : Occ. MO --> Unocc. MO Coefficients
---
55 --> 60 -0.429911

Spin Down: Occ. MO --> Unocc. MO Coefficients
---
55 --> 60 -0.429911

24 (Transition) Excitation Energy 238.8 nm
41873.9 1/cm

1 -> 25 Spin S 1.00
State Dipole 8.5091
Oscillator Strength 0.0000

State Dipole Components -8.3592 -0.0400 -1.5897
Transition Dipole Components 0.0000 -0.0000 0.0000

Spin Up : Occ. MO --> Unocc. MO Coefficients
---
56 --> 61 0.366532
55 --> 60 0.403761

Spin Down: Occ. MO --> Unocc. MO Coefficients
---
56 --> 61 0.366532
55 --> 60 0.403761

25 (Transition) Excitation Energy 231.1 nm
43270.2 1/cm

1 -> 26 Spin S 1.00
State Dipole 19.3136
Oscillator Strength 0.0000

State Dipole Components -14.5079 -12.7076 -1.0262
Transition Dipole Components 0.0000 -0.0000 0.0000

Spin Up : Occ. MO --> Unocc. MO Coefficients
---
53 --> 58 -0.586179
53 --> 59 0.323703

Spin Down: Occ. MO --> Unocc. MO Coefficients
---
53 --> 58 -0.586179
53 --> 59 0.323703

26 (Transition) Excitation Energy 230.8 nm
43333.3 1/cm

1 -> 27 Spin S 0.00
State Dipole 19.6011
Oscillator Strength 0.0019

State Dipole Components -14.7640 -12.8506 -1.0432
Transition Dipole Components -0.0895 0.2559 -0.1426

Spin Up : Occ. MO --> Unocc. MO Coefficients
---
53 --> 58 0.592802
53 --> 59 -0.329977

Spin Down: Occ. MO --> Unocc. MO Coefficients
---
53 --> 58 -0.592802
53 --> 59 0.329977

27 (Transition) Excitation Energy 229.3 nm
43614.1 1/cm

1 -> 28 Spin S 1.00
State Dipole 11.1891
Oscillator Strength 0.0000

State Dipole Components -7.5131 -8.2228 -1.0649
Transition Dipole Components -0.0000 -0.0000 -0.0000

Spin Up : Occ. MO --> Unocc. MO Coefficients
---
56 --> 62 -0.622067

Spin Down: Occ. MO --> Unocc. MO Coefficients
---
56 --> 62 -0.622067

28 (Transition) Excitation Energy 223.0 nm
44837.0 1/cm

1 -> 29 Spin S -0.00
State Dipole 7.0497
Oscillator Strength 0.2056

State Dipole Components -5.4276 -4.3807 -1.0243
Transition Dipole Components 2.2284 -2.1712 0.2636

Spin Up : Occ. MO --> Unocc. MO Coefficients
---
56 --> 60 -0.333974
56 --> 61 -0.454198

Spin Down: Occ. MO --> Unocc. MO Coefficients
---
56 --> 60 0.333974
56 --> 61 0.454198

29 (Transition) Excitation Energy 222.2 nm
44998.7 1/cm

1 -> 30 Spin S 1.00
State Dipole 4.8727
Oscillator Strength 0.0000

State Dipole Components -2.5699 -4.0376 -0.9148
Transition Dipole Components 0.0000 -0.0000 0.0000

Spin Up : Occ. MO --> Unocc. MO Coefficients
---
55 --> 61 -0.544398

Spin Down: Occ. MO --> Unocc. MO Coefficients
---
55 --> 61 -0.544398

30 (Transition) Excitation Energy 216.7 nm
46147.8 1/cm

1 -> 31 Spin S -0.00
State Dipole 7.5052
Oscillator Strength 0.1029

State Dipole Components -7.0356 -2.2131 -1.3894
Transition Dipole Components -1.1561 1.8380 -0.1716

Spin Up : Occ. MO --> Unocc. MO Coefficients
---
56 --> 60 0.353841
55 --> 60 -0.570168

Spin Down: Occ. MO --> Unocc. MO Coefficients
---
56 --> 60 -0.353841
55 --> 60 0.570168

31 (Transition) Excitation Energy 211.7 nm
47238.5 1/cm

1 -> 32 Spin S 1.00
State Dipole 7.6657
Oscillator Strength 0.0000

State Dipole Components 7.5391 0.9217 1.0369
Transition Dipole Components 0.0000 -0.0000 0.0000

Spin Up : Occ. MO --> Unocc. MO Coefficients
---
54 --> 58 -0.354472
54 --> 61 -0.336246
54 --> 62 0.415902

Spin Down: Occ. MO --> Unocc. MO Coefficients
---
54 --> 58 -0.354472
54 --> 61 -0.336246
54 --> 62 0.415902

32 (Transition) Excitation Energy 209.6 nm
47704.5 1/cm

1 -> 33 Spin S 0.00
State Dipole 5.8230
Oscillator Strength 0.0169

State Dipole Components 5.5692 1.5210 0.7601
Transition Dipole Components -0.8260 -0.2363 -0.1236

Spin Up : Occ. MO --> Unocc. MO Coefficients
---
54 --> 58 0.329315
54 --> 61 0.323946
54 --> 62 -0.408613

Spin Down: Occ. MO --> Unocc. MO Coefficients
---
54 --> 58 -0.329315
54 --> 61 -0.323946
54 --> 62 0.408613

33 (Transition) Excitation Energy 205.4 nm
48675.8 1/cm

1 -> 34 Spin S 0.00
State Dipole 8.5872
Oscillator Strength 0.0323

State Dipole Components -8.3897 -1.2521 -1.3360
Transition Dipole Components 0.9165 0.7563 -0.0100

Spin Up : Occ. MO --> Unocc. MO Coefficients
---
56 --> 60 -0.389725

Spin Down: Occ. MO --> Unocc. MO Coefficients
---
56 --> 60 0.389725

34 (Transition) Excitation Energy 203.5 nm
49142.2 1/cm

1 -> 35 Spin S 1.00
State Dipole 14.3991
Oscillator Strength 0.0000

State Dipole Components -12.1234 7.4108 -2.3319
Transition Dipole Components -0.0000 -0.0000 -0.0000

Spin Up : Occ. MO --> Unocc. MO Coefficients
---
56 --> 60 0.525382
56 --> 61 -0.322096

Spin Down: Occ. MO --> Unocc. MO Coefficients
---
56 --> 60 0.525382
56 --> 61 -0.322096

35 (Transition) Excitation Energy 202.0 nm
49515.5 1/cm

1 -> 36 Spin S 1.00
State Dipole 9.8996
Oscillator Strength 0.0000

State Dipole Components 5.0666 -8.4764 0.6946
Transition Dipole Components -0.0000 -0.0000 0.0000

Spin Up : Occ. MO --> Unocc. MO Coefficients
---
55 --> 62 -0.408660
54 --> 59 -0.415605

Spin Down: Occ. MO --> Unocc. MO Coefficients
---
55 --> 62 -0.408660
54 --> 59 -0.415605

36 (Transition) Excitation Energy 201.7 nm
49577.1 1/cm

1 -> 37 Spin S 1.00
State Dipole 5.1697
Oscillator Strength 0.0000

State Dipole Components 4.4027 -2.6802 0.3972
Transition Dipole Components 0.0000 -0.0000 -0.0000

Spin Up : Occ. MO --> Unocc. MO Coefficients
---
55 --> 62 -0.358318
54 --> 59 0.431762

Spin Down: Occ. MO --> Unocc. MO Coefficients
---
55 --> 62 -0.358318
54 --> 59 0.431762

37 (Transition) Excitation Energy 201.5 nm
49628.5 1/cm

1 -> 38 Spin S 0.00
State Dipole 13.1494
Oscillator Strength 0.0010

State Dipole Components 6.8880 11.1940 0.3948
Transition Dipole Components -0.0720 0.1908 0.0392

Spin Up : Occ. MO --> Unocc. MO Coefficients
---
54 --> 59 -0.598187

Spin Down: Occ. MO --> Unocc. MO Coefficients
---
54 --> 59 0.598187

38 (Transition) Excitation Energy 193.0 nm
51814.3 1/cm

1 -> 39 Spin S -0.00
State Dipole 8.5843
Oscillator Strength 0.0042

State Dipole Components -2.4993 -8.1898 -0.6086
Transition Dipole Components -0.4151 -0.0367 -0.0049

Spin Up : Occ. MO --> Unocc. MO Coefficients
---
56 --> 61 -0.356517
55 --> 61 0.450956

Spin Down: Occ. MO --> Unocc. MO Coefficients
---
56 --> 61 0.356517
55 --> 61 -0.450956

39 (Transition) Excitation Energy 184.5 nm
54196.3 1/cm

1 -> 40 Spin S 0.00

State Dipole 7.2060
Oscillator Strength 0.7440

State Dipole Components -3.3940 -6.3019 -0.8329
Transition Dipole Components -4.6485 -2.7493 -0.1559

Spin Up : Occ. MO --> Unocc. MO Coefficients
---
56 --> 62 0.483411
55 --> 61 0.451634

Spin Down: Occ. MO --> Unocc. MO Coefficients
---
56 --> 62 -0.483411
55 --> 61 -0.451634

40 (Transition) Excitation Energy 183.8 nm
54400.4 1/cm

1 -> 41 Spin S 1.00
State Dipole 18.1635
Oscillator Strength 0.0000

State Dipole Components -14.0168 -11.5095 -0.9867
Transition Dipole Components 0.0000 0.0000 0.0000

Spin Up : Occ. MO --> Unocc. MO Coefficients
---
53 --> 60 0.630478

Spin Down: Occ. MO --> Unocc. MO Coefficients
---
53 --> 60 0.630478

41 (Transition) Excitation Energy 183.7 nm
54440.3 1/cm

1 -> 42 Spin S -0.00
State Dipole 18.0418
Oscillator Strength 0.0151

State Dipole Components -13.9164 -11.4396 -0.9884
Transition Dipole Components -0.6126 -0.4484 -0.1162

Spin Up : Occ. MO --> Unocc. MO Coefficients
---
53 --> 60 -0.626683

Spin Down: Occ. MO --> Unocc. MO Coefficients
---
53 --> 60 0.626683

42 (Transition) Excitation Energy 182.1 nm
54900.4 1/cm

1 -> 43 Spin S -0.00
State Dipole 15.5799
Oscillator Strength 0.2167

State Dipole Components 0.4389 -15.5737 -0.0109
Transition Dipole Components 1.0788 -2.6839 0.1588

Spin Up : Occ. MO --> Unocc. MO Coefficients
---
55 --> 62 0.616977

Spin Down: Occ. MO --> Unocc. MO Coefficients
---
55 --> 62 -0.616977

43 (Transition) Excitation Energy 178.7 nm
55955.7 1/cm

1 -> 44 Spin S 1.00
State Dipole 15.5238
Oscillator Strength 0.0000

State Dipole Components 1.9807 15.3950 -0.2438
Transition Dipole Components -0.0000 0.0000 0.0000

Spin Up : Occ. MO --> Unocc. MO Coefficients
---
54 --> 60 -0.476278

Spin Down: Occ. MO --> Unocc. MO Coefficients
---
54 --> 60 -0.476278

44 (Transition) Excitation Energy 178.5 nm
56027.6 1/cm

1 -> 45 Spin S 0.00
State Dipole 15.0165
Oscillator Strength 0.0042

State Dipole Components 2.0402 14.8756 -0.2249
Transition Dipole Components 0.3237 -0.2269 -0.0359

Spin Up : Occ. MO --> Unocc. MO Coefficients
---
54 --> 60 -0.477435

Spin Down: Occ. MO --> Unocc. MO Coefficients
---
54 --> 60 0.477435

45 (Transition) Excitation Energy 166.4 nm
60112.2 1/cm

1 -> 46 Spin S 1.00
State Dipole 16.9477
Oscillator Strength 0.0000

State Dipole Components -7.0509 -15.4106 -0.1532
Transition Dipole Components 0.0000 -0.0000 0.0000

Spin Up : Occ. MO --> Unocc. MO Coefficients
---
53 --> 61 -0.548997

Spin Down: Occ. MO --> Unocc. MO Coefficients
---
53 --> 61 -0.548997

46 (Transition) Excitation Energy 166.2 nm
60176.8 1/cm

1 -> 47 Spin S 0.00
State Dipole 17.0378
Oscillator Strength 0.0008

State Dipole Components -7.0625 -15.5043 -0.1502
Transition Dipole Components -0.0094 0.1569 -0.0522

Spin Up : Occ. MO --> Unocc. MO Coefficients
---
53 --> 61 0.550959

Spin Down: Occ. MO --> Unocc. MO Coefficients
---
53 --> 61 -0.550959

47 (Transition) Excitation Energy 161.2 nm
62036.8 1/cm

1 -> 48 Spin S 1.00
State Dipole 12.8527
Oscillator Strength 0.0000

State Dipole Components 2.6981 12.5661 -0.0866
Transition Dipole Components 0.0000 0.0000 0.0000

Spin Up : Occ. MO --> Unocc. MO Coefficients
---
54 --> 61 0.389539
54 --> 62 0.381649

Spin Down: Occ. MO --> Unocc. MO Coefficients
---
54 --> 61 0.389539
54 --> 62 0.381649

48 (Transition) Excitation Energy 161.0 nm
62127.5 1/cm

1 -> 49 Spin S 0.00
State Dipole 12.7635
Oscillator Strength 0.0033

State Dipole Components 2.7269 12.4685 -0.0851
Transition Dipole Components -0.3269 -0.0730 0.0294

Spin Up : Occ. MO --> Unocc. MO Coefficients
---
54 --> 61 0.389623
54 --> 62 0.385891

Spin Down: Occ. MO --> Unocc. MO Coefficients
---
54 --> 61 -0.389623
54 --> 62 -0.385891

49 (Transition) Excitation Energy 152.8 nm
65465.5 1/cm

1 -> 50 Spin S 1.00
State Dipole 33.7380
Oscillator Strength 0.0000

State Dipole Components -9.6586 -32.3217 0.5216
Transition Dipole Components -0.0000 0.0000 -0.0000

Spin Up : Occ. MO --> Unocc. MO Coefficients
---
53 --> 61 -0.332050
53 --> 62 0.608711

Spin Down: Occ. MO --> Unocc. MO Coefficients
---
53 --> 61 -0.332050
53 --> 62 0.608711

50 (Transition) Excitation Energy 152.6 nm
65544.3 1/cm

1 -> 51 Spin S 0.00
State Dipole 33.7109
Oscillator Strength 0.0007

State Dipole Components -9.6627 -32.2922 0.5199
Transition Dipole Components 0.0850 -0.0999 0.0632

Spin Up : Occ. MO --> Unocc. MO Coefficients
---
53 --> 61 0.329521
53 --> 62 -0.610348

Spin Down: Occ. MO --> Unocc. MO Coefficients
---
53 --> 61 -0.329521
53 --> 62 0.610348

****

Energy=-17839.355974 Gradient=197.913195 Symmetry=C1

ENERGIES AND GRADIENT
Total Energy = -101792.8077100 (kcal/mol)
Total Energy = -162.213925872 (a.u.)
Binding Energy = -17839.3559741 (kcal/mol)
Isolated Atomic Energy = -83953.4517358 (kcal/mol)
Electronic Energy = -573309.5335678 (kcal/mol)
Core-Core Interaction = 471516.7258578 (kcal/mol)
CI Energy = 0.0000000 (kcal/mol)
Number of Configurations Used = 51
Heat of Formation = -13471.5859741 (kcal/mol)
Gradient of Reference Configuration = 197.9131955 (kcal/mol/Ang)

MOLECULAR POINT GROUP
C1

EIGENVALUES OF THE REFERENCE CONFIGURATION(eV)
Symmetry: 1 A 2 A 3 A 4 A 5 A
Eigenvalue: -54.773384 -49.352470 -48.786316 -47.826180 -45.703484

Symmetry: 6 A 7 A 8 A 9 A 10 A
Eigenvalue: -42.437500 -41.634308 -39.909592 -38.372990 -35.460918

Symmetry: 11 A 12 A 13 A 14 A 15 A
Eigenvalue: -34.781673 -34.722301 -34.172939 -32.612568 -31.477646

Symmetry: 16 A 17 A 18 A 19 A 20 A
Eigenvalue: -31.327703 -29.181995 -28.810131 -27.402082 -26.127823

Symmetry: 21 A 22 A 23 A 24 A 25 A
Eigenvalue: -25.817547 -24.705961 -24.049934 -23.131914 -23.097416

Symmetry: 26 A 27 A 28 A 29 A 30 A
Eigenvalue: -22.687613 -22.092476 -21.633503 -21.513481 -20.476183

Symmetry: 31 A 32 A 33 A 34 A 35 A
Eigenvalue: -20.341412 -19.797405 -19.629141 -19.026590 -18.658081

Symmetry: 36 A 37 A 38 A 39 A 40 A
Eigenvalue: -18.543922 -18.258272 -18.172812 -17.974449 -17.518076

Symmetry: 41 A 42 A 43 A 44 A 45 A
Eigenvalue: -17.283987 -17.250700 -16.935650 -16.864218 -16.298143

Symmetry: 46 A 47 A 48 A 49 A 50 A
Eigenvalue: -15.939537 -15.658021 -15.430650 -15.215533 -14.624290

Symmetry: 51 A 52 A 53 A 54 A 55 A
Eigenvalue: -13.903387 -13.282524 -13.109770 -12.741471 -11.973325

Symmetry: 56 A 57 A 58 A 59 A 60 A
Eigenvalue: -11.843259 -10.112464 -4.770159 -4.028529 -3.354715

Symmetry: 61 A 62 A 63 A 64 A 65 A
Eigenvalue: -2.486293 -2.288451 -1.996456 -1.417881 -1.178719

Symmetry: 66 A 67 A 68 A 69 A 70 A
Eigenvalue: -1.061931 -0.802159 -0.482724 -0.252934 0.007641

Symmetry: 71 A 72 A 73 A 74 A 75 A
Eigenvalue: 0.186533 0.197685 0.554564 0.768398 1.066390

Symmetry: 76 A 77 A 78 A 79 A 80 A
Eigenvalue: 1.071543 1.088024 1.762438 1.868326 2.136314

Symmetry: 81 A 82 A 83 A 84 A 85 A
Eigenvalue: 2.572968 2.767962 2.886609 3.190971 3.321578

Symmetry: 86 A 87 A 88 A 89 A 90 A
Eigenvalue: 3.467420 3.589502 3.692306 3.898882 3.919411

Symmetry: 91 A 92 A 93 A 94 A 95 A
Eigenvalue: 4.795054 4.935461 5.269394 5.762344 6.263196

Symmetry: 96 A 97 A 98 A 99 A 100 A
Eigenvalue: 6.671063 6.862059 7.494579 7.771515 7.953640

Symmetry: 101 A 102 A 103 A 104 A 105 A
Eigenvalue: 8.092816 8.808935 9.030408 9.414911 9.790030

Symmetry: 106 A 107 A 108 A
Eigenvalue: 10.036507 10.486177 11.079528

ATOMIC ORBITAL ELECTRON POPULATIONS
AO: 1 S C 1 Px C 1 Py C 1 Pz C 2 S C
1.083562 0.976814 0.850903 1.033070 1.076551

AO: 2 Px C 2 Py C 2 Pz C 3 S C 3 Px C
0.982147 0.960257 0.961322 1.085276 0.964751

AO: 3 Py C 3 Pz C 4 S C 4 Px C 4 Py C
0.987396 0.936972 1.076594 0.949256 0.977780

AO: 4 Pz C 5 S C 5 Px C 5 Py C 5 Pz C
0.991451 1.051475 0.905057 0.930951 1.034173

AO: 6 S C 6 Px C 6 Py C 6 Pz C 7 S C
1.046113 0.865955 0.962704 1.066773 1.083735

AO: 7 Px C 7 Py C 7 Pz C 8 S C 8 Px C
0.957540 0.969166 0.978238 1.044494 0.970781

AO: 8 Py C 8 Pz C 9 S C 9 Px C 9 Py C
0.941873 0.994853 1.043257 0.952007 0.976366

AO: 9 Pz C 10 S C 10 Px C 10 Py C 10 Pz C
1.002009 1.044124 0.963905 0.864867 1.050425

AO: 11 S N 11 Px N 11 Py N 11 Pz N 12 S N
1.236099 1.165825 1.106466 1.538145 1.219724

AO: 12 Px N 12 Py N 12 Pz N 13 S C 13 Px C
1.146914 1.132412 1.531317 1.099379 0.979276

AO: 13 Py C 13 Pz C 14 S C 14 Px C 14 Py C
0.971042 0.950729 1.082150 0.988690 0.963044

AO: 14 Pz C 15 S C 15 Px C 15 Py C 15 Pz C
0.958878 1.084556 0.958508 0.964655 1.025796

AO: 16 S C 16 Px C 16 Py C 16 Pz C 17 S C
1.086276 0.956444 0.996906 0.948131 1.010979

AO: 17 Px C 17 Py C 17 Pz C 18 S N 18 Px N
0.859559 0.845771 0.962754 1.320428 1.230160

AO: 18 Py N 18 Pz N 19 S C 19 Px C 19 Py C
1.586830 1.130072 1.041945 0.998606 0.967112

AO: 19 Pz C 20 S C 20 Px C 20 Py C 20 Pz C
0.917392 1.041489 0.991545 0.981033 0.910922

AO: 36 S C 36 Px C 36 Py C 36 Pz C 37 S O
1.053840 0.834585 0.928247 0.697428 1.701541

AO:	37 Px O	37 Py O	37 Pz O	39 S O	39 Px O
	1.265351	1.497883	1.843832	1.835892	1.835294

AO:	39 Py O	39 Pz O	24 S H	25 S H	26 S H
	1.371066	1.491885	0.979465	0.983506	0.967599

AO:	27 S H	28 S H	29 S H	30 S H	31 S H
	0.944945	0.952637	0.950494	0.940112	0.950693

AO:	32 S H	33 S H	34 S H	35 S H	21 S H
	0.933604	0.953695	0.960816	0.962555	0.968089

AO:	22 S H	38 S H	23 S H
	0.983582	0.749287	0.979174

NET CHARGES AND COORDINATES

Atom	Z	Charge	Coordinates(Angstrom) x	y	z	Mass
1	6	0.055652	1.50729	-3.81051	0.27028	12.01100
2	6	0.019723	2.76862	-4.36357	0.38643	12.01100
3	6	0.025604	3.91833	-3.57264	0.41792	12.01100
4	6	0.004919	3.77408	-2.17789	0.32341	12.01100
5	6	0.078344	2.51610	-1.62592	0.19369	12.01100
6	6	0.058455	2.04898	-0.25856	0.05925	12.01100
7	6	0.011322	2.75335	0.92001	0.00959	12.01100
8	6	0.047999	2.07652	2.16071	-0.09265	12.01100
9	6	0.026360	0.64877	2.13580	-0.17355	12.01100
10	6	0.076678	-0.09081	0.91790	-0.15626	12.01100
11	7	-0.046535	0.63507	-0.30015	-0.02661	14.00700
12	7	-0.030367	1.35751	-2.43107	0.17235	14.00700
13	6	-0.000427	-0.10711	3.32771	-0.28437	12.01100
14	6	0.007237	-1.48960	3.33078	-0.37218	12.01100
15	6	-0.033514	-1.47707	0.90742	-0.26502	12.01100
16	6	0.012243	-2.17309	2.11218	-0.37131	12.01100
17	6	0.320937	0.24605	-1.62256	0.05046	12.01100
18	7	-0.267491	-1.08382	-2.03168	0.01379	14.00700
19	6	0.074945	-1.43283	-2.79693	-1.14130	12.01100
20	6	0.075012	-1.55691	-2.61722	1.22876	12.01100
36	6	0.485899	2.83058	3.38734	-0.11900	12.01100
37	8	-0.308607	4.12854	3.25085	-0.49883	15.99900
39	8	-0.534137	2.38816	4.51980	0.26988	15.99900
24	1	0.020535	-1.16045	-3.63049	1.38746	1.00800
25	1	0.016494	-1.27639	-1.99369	2.09021	1.00800
26	1	0.032401	-2.65423	-2.67551	1.19053	1.00800
27	1	0.055055	4.91237	-4.02008	0.51939	1.00800
28	1	0.047363	4.63574	-1.50364	0.34921	1.00800
29	1	0.049506	2.83312	-5.45396	0.45936	1.00800
30	1	0.059888	0.56797	-4.37277	0.23454	1.00800
31	1	0.049307	3.84588	0.87047	0.06287	1.00800
32	1	0.066396	0.46239	4.26761	-0.29413	1.00800
33	1	0.046305	-2.03973	4.27315	-0.45112	1.00800
34	1	0.039184	-3.26530	2.08681	-0.45792	1.00800
35	1	0.037445	-2.00026	-0.05608	-0.24902	1.00800
21	1	0.031911	-2.53001	-2.84005	-1.20421	1.00800
22	1	0.016418	-1.04944	-2.31769	-2.05351	1.00800
38	1	0.250713	4.63977	4.13139	-0.45857	1.00800
23	1	0.020826	-1.04925	-3.82852	-1.10023	1.00800

ATOMIC GRADIENTS

Atom	Z	Gradients(kcal/mol/Angstrom) x	y	z
1	6	-51.10736	-220.46179	14.99152
2	6	66.66503	-83.31340	7.21026
3	6	83.76625	-90.78800	8.86582
4	6	65.83748	75.70012	0.69384
5	6	259.06212	85.53788	11.92066
6	6	241.98906	87.99786	7.37290
7	6	79.14595	-50.32732	3.80088
8	6	-10.29970	89.86197	1.14758
9	6	56.48413	10.10083	4.82367
10	6	-79.31520	100.55816	-11.43387
11	7	-139.46442	85.61885	-19.39728
12	7	-75.61322	-120.60224	2.54639
13	6	25.21154	70.77222	-2.80918
14	6	-62.08143	91.94165	-3.92643
15	6	-54.39813	-76.88707	-7.21908
16	6	-96.91021	14.51336	-6.58714
17	6	-132.18802	-42.71424	-6.49697
18	7	-205.15395	298.91949	-31.89387
19	6	-38.16219	-76.86720	-132.31892
20	6	-57.43547	-56.51472	133.75605
36	6	-175.29039	-275.49145	-62.29064
37	8	377.28132	-597.81599	-224.04977
39	8	-280.23946	737.25507	261.15949
24	1	132.20547	-357.35621	65.84532
25	1	93.72400	214.61781	308.77429
26	1	-387.60373	-23.31443	-5.37517
27	1	359.71927	-161.02971	36.71099
28	1	310.66625	243.59252	9.68473
29	1	22.30100	-393.56521	26.25416
30	1	-333.39237	-204.28626	-12.47470
31	1	392.78825	-19.85518	18.69972

32	1	184.21035	329.60383	-8.48562
33	1	-198.81227	340.40582	-28.33753
34	1	-392.80276	-9.61022	-31.44649
35	1	-191.14077	-331.60874	4.40464
21	1	-386.65717	-18.91985	-28.36778
22	1	130.69095	162.92206	-326.54793
38	1	338.62069	536.33524	17.47519
23	1	127.69915	-364.92550	3.32026

Dipole (Debyes)	x	y	z	Total
Point-Chg.	0.345	-9.256	-0.401	9.271
sp Hybrid	0.688	-1.026	0.124	1.241
pd Hybrid	0.000	0.000	0.000	0.000
Sum	1.033	-10.282	-0.278	10.337

HyperChem log stop -- Tue Nov 02 19:43:00 2004.